Pharmacological Research 172 (2021) 105806

Contents lists available at ScienceDirect

Pharmacological Research

journal homepage: www.elsevier.com/locate/yphrs

Invited Review

Blockade of mutant *RAS* oncogenic signaling with a special emphasis on KRAS

Robert Roskoski Jr.

Blue Ridge Institute for Medical Research, 3754 Brevard Road, Suite 106, Box 19, Horse Shoe, NC 28742-8814, United States

ARTICLE INFO

Keywords:
Cancer mutations
Non-small cell lung cancer
Pancreatic cancer
Targeted covalent inhibitors
MAP kinase signaling pathway
PI3-kinase signaling pathway

Chemical compounds studied in this article:
Adagrasib (PubChem CID: 138611145)
Belvarafenib (PubChem CID: 89655386)
Buparlisib (PubChem CID: 16654980)
Lifirafenib (PubChem CID: 89670174)
Naporafenib (PubChem CID: 90456533)
Pictilisib (PubChem CID: 17755052)
RO5126766 (PubChem CID: 16719221)
Sotorasib (PubChem CID: 137278711)
Tipifarnib (PubChem CID: 159324)
Ulixertinib (PubChem CID: 11719003)

ABSTRACT

RAS proteins (HRAS, KRAS, NRAS) participate in many physiological signal transduction processes related to cell growth, division, and survival. The RAS proteins are small (188/189 amino acid residues) and they function as GTPases. These proteins toggle between inactive and functional forms; the conversion of inactive RAS-GDP to active RAS-GTP as mediated by guanine nucleotide exchange factors (GEFs) turns the switch on and the intrinsic RAS-GTPase activity stimulated by the GTPase activating proteins (GAPs) turns the switch off. RAS is upstream to the RAS-RAF-MEK-ERK and the PI3-kinase-AKT signaling modules. Importantly, the overall incidence of *RAS* mutations in all cancers is about 19% and RAS mutants have been a pharmacological target for more than three decades. About 84% of all RAS mutations involve KRAS. Except for the GTP/GDP binding site, the RAS proteins lack other deep surface pockets thereby hindering efforts to identify high-affinity antagonists; thus, they have been considered to be undruggable. *KRAS* mutations frequently occur in lung, colorectal, and pancreatic cancers, the three most deadly cancers in the United States. Studies within the last decade demonstrated that the covalent modification of KRAS C12, which accounts for about 10% of all RAS mutations, led to the discovery of an adjacent pocket (called the switch II pocket) that accommodated a portion of the drug. This led to the development of sotorasib as a second-line treatment of $KRAS^{G12C}$-mutant non-small cell lung cancer. Considerable effort also has been expended to develop MAP kinase and PI3-kinase pathway inhibitors as indirect RAS antagonists.

1. Overview of RAS and the MAP kinase and PI3-kinase signaling pathways

RAS proteins participate in many signal transduction processes related to cell growth, division, and survival as described in studies that began in the 1960s [1]. Jennifer J Harvey working at the London Hospital Research Laboratories isolated a transforming retrovirus (Harvey sarcoma virus) from leukemic rats that was able to produce sarcomas in rodents as reported in 1964 [2]. Werner H Kirsten and LA Mayer working at the University of Chicago isolated a different (Kirsten sarcoma virus), but related, rat transforming virus [3]. *HRAS* and *KRAS,* the corresponding normal human cellular proto-oncogenes, were identified [4] from studies of these two transforming retroviruses by Edward M. Scolnick and colleagues at the National Institutes of Health [5]. In 1982, activated and transforming human *RAS* genes were discovered in human cancer cells by several groups including Geoffrey M. Cooper at Harvard [6], Robert Weinberg at the Massachusetts Institute of Technology [7], Mariano Barbacid and Stuart A. Aaronson at the National Institutes of Health [8], and Michael Wigler at the Cold Spring Harbor Laboratory [9]. A third *RAS* gene was subsequently discovered by investigators in the group of Robin Weiss at the Institute of Cancer Research [10,11] and Michael Wigler at the Cold Spring Harbor Laboratory [12] and named *NRAS*, for its initial identification in human neuroblastoma cells. Their gene symbols are *HRAS*, *KRAS,* and *NRAS;* alternative splicing of the *KRAS* gene product yields KRAS4a and KRAS4b isoforms where 4 refers to which exon 4 (a or b) is included in the final product. The three human *RAS* genes encode extremely similar proteins made up of chains of 188–189 amino acids. Gibbs et al. were the first to demonstrate that HRAS had GTPase activity and that an oncogenic variant ($HRAS^{G12V}$) exhibited only one-third of the GTPase specific activity as the wild type

Abbreviations: CRC, colorectal cancer; EGFR, epidermal growth factor receptor; GAP, GTPase activating protein; GEF, guanine nucleotide exchange factor; GPCR, G-protein coupled receptor; MAPK, mitogen activated protein kinase; NSCLC, non-small cell lung cancer; PDGFR, platelet-derived growth factor receptor; pERK, phosphorylated ERK; PI3K, phosphatidylinositol 3-kinase; PIP3, phosphatidylinositol-3,4,5-trisphosphate; RBD, RAS-binding domain; Ro5, Lipinski's rule of five; S-I, switch I; S-IIP, switch-II pocket; VEGFR, vascular endothelial growth factor receptor.

E-mail address: rrj@brimr.org.

https://doi.org/10.1016/j.phrs.2021.105806
Received 7 August 2021; Accepted 7 August 2021
Available online 24 August 2021

enzyme [13].

The RAS-RAF-MEK-ERK MAPK (mitogen activated protein kinase) and PI3K (phosphatidylinositol 3-kinase) AKT-mTOR signaling modules are among the most important physiological signal transduction pathways as well as significant oncogenic drivers of human malignancies [14–25]. These evolutionarily conserved pathways transmit extracellular signals (growth factors, cytokines) to intracellular signaling modules. Significantly, the MAP kinase and PI3-kinase pathways are activated by many of the same transmembrane receptors. For example, activated EGFR becomes auto-phosphorylated at specific tyrosine residues that interact with guanine nucleotide exchange factors (GEFs) such as SOS (from *Drosophila* Son Of Sevenless) as well as other adapter proteins such as GRB2 (Growth factor Receptor Bound protein 2). These factors facilitate the conversion of dormant RAS-GDP to the functional and active RAS-GTP in the plasma membrane [26–30]. These RAS proteins toggle between inactive and functional forms; the conversion of inactive RAS-GDP to active RAS-GTP turns the switch on and the intrinsic RAS-GTPase activity stimulated by the GTPase activating proteins (GAPs) such as NF1 (neurofibromin-1) turns the switch off (Fig. 1). Note that much of the PI3-kinase and RAS biochemistry and signaling occurs within the inner leaflet of the plasma membrane [29].

To activate the MAP kinase module, RAS-GTP promotes the creation of functional homodimers or heterodimers composed of A/B/CRAF by a complex process (the RAF acronym corresponds to *R*apidly *A*ccelerated *F*ibrosarcoma, initially described in mice) [14,15]. The RAF enzymes are protein-serine/threonine kinases that mediate the ATP-dependent phosphorylation and activation of MEK1 and MEK2 (*M*AP/*E*RK *K*inase). The activated MEK protein kinases then mediate the phosphorylation and activation of ERK1 and ERK2 (*E*xtracellular Signal-*R*egulated protein *K*inases). The A/B/CRAF and MEK1/2 protein kinases have restricted substrate specificities [15,17]. Consequently, the only documented RAF substrates are MEK1/2 and the only documented MEK1/2 substrates are ERK1/2. In contrast to the RAF and MEK enzyme families, ERK1/2 have broad substrate specificity and they mediate the phosphorylation of literally hundreds of different cytosolic and nuclear proteins [19,31]. Accordingly, the linear MAP kinase module branches extensively at the ERK1/2 node (Fig. 2). The Kinase Suppressors of RAS (KSR1/2) are the closest relatives of the RAF family kinases (www.kinase.com/human/kinome). KSR1/2 are impaired protein kinases (but not kinase dead) that function as scaffolds to assemble RAF, MEK, and ERK to regulate signaling efficiency [19,31]. Components of the MAP kinase pathway including GEFs, GAPs, and protein kinases are listed in Table 1.

PI3-kinases mediate the phosphorylation of phosphatidylinositol-4,5-bisphosphate (PI-4,5-P2) to generate phosphatidylinositol-3,4,5-trisphosphate (PIP3) according to the following chemical equation:

PI-4,5-P2 + ATP → PI-3,4,5-P3 + ADP

These enzymes are divided into three classes: class I PI3-kinases mediate the conversion of PI-4,5-P2 to PIP3 and include the isoforms that are most frequently mutated in cancer. The class II PI3-kinases mediate the conversion of PI-4-P to PI-3,4-P2; this phospholipid occurs on early endosomes and participates in AKT protein kinase signaling [32,33]. Class III PI3-kinases catalyze the conversion of PI to PI-3-P, a major phospholipid that participates in autophagy and vesicular trafficking [34,35]. The class III Vps34 was first identified in budding yeast (*Saccharomyces cerevisiae)* as a protein involved in vesicle-mediated Vacuolar protein sorting (Vps) and *vps34* refers to a complementation group name. Table 2 summarizes the properties of the three classes of PI3-kinases.

The class I PI3-kinases are made up of p110 catalytic subunits that are encoded by four genes (*PIK3CA*, *PIK3CB*, *PIK3CD*, and *PIK3CG*) that correspond to the p110α, p110β, p110δ, and p110γ isoforms, respectively [36]. These catalytic subunits are constitutively bound to regulatory subunits that are encoded by five genes (*PIK3R1*, *PIK3R2*, *PIK3R3*, *PIK3R5*, and *PIK3R6*) that correspond to the p85α, p85β, p55γ, p101, and p87 proteins (Table 2). The p85/p55 regulatory subunits form dimers with p110α or p110δ catalytic subunits thereby forming complexes that are regulated chiefly by receptor protein-tyrosine kinases. In contrast, the p101 and p87 regulatory subunits heterodimerize with p110γ to form complexes that are regulated mainly by G protein-coupled receptors (GPCRs). Complexes containing the p110β catalytic subunit

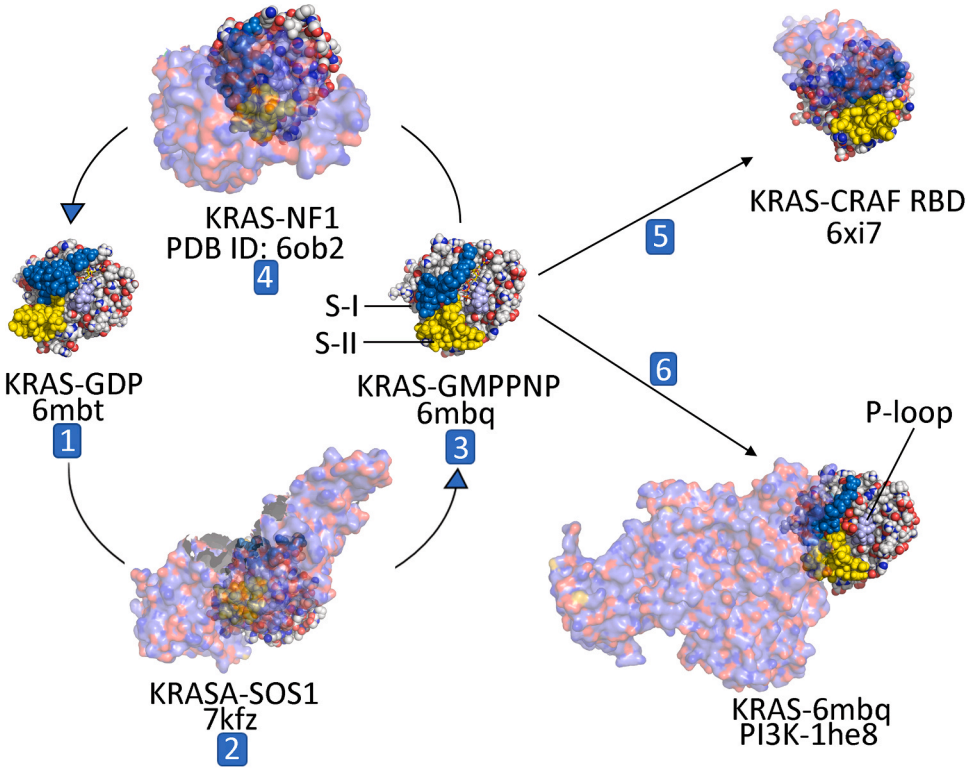

Fig. 1. The RAS cycle and RAS effector pathways. The inactive GDP state (1) interacts with SOS1 (2) leading to the exchange of GTP for GDP and the formation of the active RAS-GTP complex (3). Conversion to the inactive GDP state is mediated by GAPs such as NF1 (4). The active RAS-GTP state leads to the activation of the MAP kinase pathway (5) or the PI3-kinase pathway (6). The regulatory and effector proteins are depicted as semi-transparent spheres. The switch I regions are colored blue; switch II, yellow, and P-loop, gray. This figure and 3B, 4A, 6, and 8B/C/E/F/H/I were prepared using the PyMOL Molecular Graphics System Version 1.5.0.4 Schrödinger, LLC.

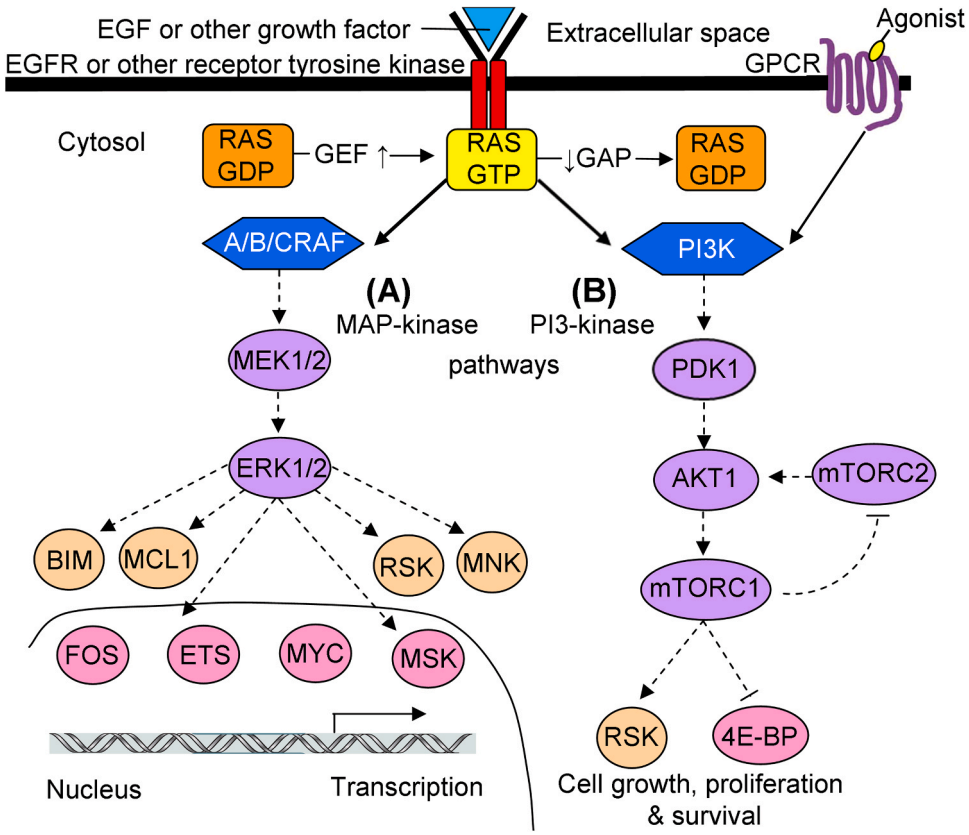

Fig. 2. Schematic diagram illustrating the activation of the MAP kinase (A) and PI3-kinase pathways (B) by RAS-GTP.

are activated by receptor protein-tyrosine kinases as well as GPCRs. The p85/p55 regulatory subunits contain an N-terminal SH2 domain (nSH2), a C-terminal SH2 domain (cSH2), and an inter-SH2 (iSH2) coiled-coil domain that mediates the interaction with the various catalytic subunits [25]. The SH2 domains bind to pYxxM amino acid motifs of activated receptor protein-tyrosine kinases or their adapter proteins that result in the recruitment of PI3-kinases to the plasma membrane where their substrate (PI-4,5-P2) is abundant and triggers conformational changes that enhance PI3-kinase catalytic activity [37,38]. The class I and class II PI3-kinases contain a RAS-binding domain (RBD) that participates in the regulation of these enzymes.

Following receptor protein-tyrosine kinase activation by its stimulatory ligand, the activated receptor, its adapter proteins, or both undergo tyrosine phosphorylation at multiple YxxM motifs that interact with the SH2 domains of the p85 PI3-kinase regulatory subunits to alter the PI3-kinase catalytic subunit conformation while attracting it to the substrate-rich plasma membrane, a process that results in the biosynthesis of PIP3 [20]. Furthermore, the AKT protein kinase is activated following its binding to PIP3 within the plasma membrane to mediate downstream growth and survival pathways (Fig. 2). PIP3 signaling is terminated by phospholipid phosphatases. PIP3 is converted to PI-4, 5-P2 following the hydrolysis catalyzed by PTEN (phosphatase and tensin homolog) or it is converted to PI-3,4-P2 in a reaction catalyzed by Ship2 (phosphatidyl-3,4,5-trisphosphate 5-phosphatase) [39].

CXCR4, a member of the family of chemokine-activated GPCRs, is expressed in immune response cells. This receptor is involved in both cancer development and progression and is implicated in the pathophysiology of small lymphocytic lymphoma and chronic lymphocytic leukemia [40]. Furthermore, many cancer cells express higher levels of CXCR4 when compared with their normal cellular counterparts. Activation of PI3-kinase by GPCRs such as CXCR4 is mediated by the Gβ/γ subunit that activates both p110β and p110γ by a mechanism that is unclear [36]. The activation of p110β and p110γ by CXCR leads to the stimulation of AKT protein kinase activity.

PIP3, which is generated by PI3-kinase, binds to the amino-terminal PH (pleckstrin homology) domain of AKT1 and attracts it to the plasma membrane [20–22]. AKT1 is activated following its phosphorylation at (i) T308 as catalyzed by PDK1 (*P*hosphoinositide-*D*ependent protein *K*inase-1) and (ii) S473 as catalyzed by mTORC2 (mammalian target of rapamycin complex 2). AKT1, in turn, leads to the activation of mTORC1. PDK1, AKT1, and mTORC1/2 are protein-serine/threonine kinases. mTORC1 participates in the regulation of ribosomal S6 kinase (S6K) and 4E-BP (eukaryotic translation initiation factor 4E). AKT1 and mTORC1 protein kinases promote protein synthesis, cell growth, proliferation, survival, and angiogenesis [22]. The existence of parallel pathways downstream from activated receptors and oncogenes suggests a strategy of combining targeted inhibitors of RAF, MEK, or ERK of the MAP kinase pathway along with inhibition of PI3-kinase, AKT1/PKB, or mTOR of the PI3K pathway in the treatment of various neoplasms [41]. Components of the PI3-kinase pathway are listed in Table 3.

2. Oncogenic mutations in the RAS and PI3-kinase pathways

Prior et al. found that the overall incidence of *RAS* mutations in all cancers is about 19% [42]. They converted the *RAS* mutation frequencies found in cancer genetic databases with the number of patients with each type of tumor to arrive at this value. The total number of *HRAS* mutations in the 29 most common cancers in the United States was about 18,000, that for *KRAS* was about 202,000, and that for *NRAS* was about 44,000. The highest annual incidence of *HRAS* mutations occurred in bladder cancer (5700) and head and neck squamous cell carcinoma (3300) and the highest incidence of *NRAS* mutations occurred in skin cutaneous melanoma (15,000) and multiple myeloma (6000). In the case of *KRAS* mutations, the greatest incidence occurred in colon and pancreatic adenocarcinomas (each with about 49,000 cases per year), lung adenocarcinoma (30,000), rectal adenocarcinoma (26,

Table 1
RAS and MAP kinase pathway components.

Component	UniprotKB no.	No. of amino acids	MW (kDa)	Comments from UniProt
Receptor protein-tyrosine kinases				Many
HRAS	P01112	189	21.3	GTPase
KRAS4a	P01116-1	189	21.7	GTPase; an alternative splice form
KRAS4b	P01116-2	188	21.4	GTPase; an alternative splice form
NRAS	P01111	189	21.2	GTPase
GEFs; guanine-nucleotide exchange factors				
SOS1	Q07889	1333	152.4	Son of sevenless homolog 1
SOS2	Q07890	1332	153.0	Son of sevenless homolog 2
GRB2	P62993	217	25.2	Growth factor receptor-bound protein 2
RASGRP1	O95267	797	90.4	RAS guanyl-releasing protein 1; exchange factor for H/K/NRAS
RASGRP2	Q7LDG7	609	69.2	RAS guanyl-releasing protein 2; exchange factor for RRAS, RRAS2, NRAS, KRAS but not HRAS
RASGRP3	Q8IV61	690	78.3	RAS guanyl-releasing protein 3; exchange factor for H/K/NRAS and RAP1
RASGRP4	Q8TDF6	673	74.9	RAS guanyl-releasing protein 4; exchange factor for H/K/NRAS
RAPGEF1	Q13905	1077	120.5	RAP guanine nucleotide exchange factor 1; activates H/K/NRAS and RAP1
RAPGEF2	Q9Y4G8	1499	167.4	RAP guanine nucleotide exchange factor 2; activates H/K/NRAS and RAP1
RASGRF1	Q13972	1273	145.2	RAS-specific guanine nucleotide-releasing factor 1 aka CDC25; activates H/K/NRAS
RASGRF2	O14827	1237	140.8	RAS-specific guanine nucleotide-releasing factor 2 that is regulated by calcium ion; activates H/K/NRAS and RAC1
GAPs; inhibitory regulators of the RAS pathway				
RASA1	P20936	1047	116.4	RAS GTPase-activating protein 1; stimulates the GTPase of normal but not oncogenic RAS
RASA2	Q15283	850	96.6	RAS GTPase-activating protein 2
RASA3	Q14644	834	95.7	RAS GTPase-activating protein 3
RASAL1	O95294	804	90.0	RAS GAP-activating-like protein 1
RASAL2	Q9UJF2	1139	128.6	RAS GTPase-activating protein nGAP
RASAL3	Q86YV0	1011	111.9	RAS GAP-activating-like protein 3
DAB2IP	Q5VWQ8	1189	131.6	Disabled homolog 2-interacting protein; acts as a GTPase-activating protein (GAP) for the ADP ribosylation factor 6 (ARF6) and RAS proteins
NF1	P21359	2839	319.4	Neurofibromin 1; stimulates GTPase activity of RAS proteins
SPRED1	Q7Z699	444	50.4	Sprouty-related, EVH1 domain-containing protein 1; works in conjunction with NF1
SPRED2	Q7Z698	418	47.6	Sprouty-related, EVH1 domain-containing protein 2; works in conjunction with NF1
SPRED3	Q2MJR0	408	42.8	Sprouty-related, EVH1 domain-containing protein 3; works in conjunction with NF1
SYNGAP1	Q96PV0	1343	148.3	RAS/RAP GTPase-activating protein SYNGAP
Protein kinases				
ARAF	P10398	606	67.6	Rapidly accelerated fibrosarcoma; mediates the phosphorylation of MEK1/2
BRAF	P15056	766	84.4	Mediates the phosphorylation of MEK1/2
CRAF	P04049	648	73.0	Mediates the phosphorylation of MEK1/2
MEK1	Q02750	393	43.4	*M*EK/*E*RK *K*inase; dual specificity mitogen-activated protein kinase kinase 1 corresponding to the *MAP2K1* gene
MEK2	P36507	400	44.4	Dual specificity mitogen-activated protein kinase kinase 2 corresponding to the *MAP2K2* gene
KSR1	Q8IVT5	923	102.1	Kinase suppressor of RAS 1; dimerizes with BRAF and promotes BRAF-mediated phosphorylation of MEK1 and MEK2
KSR2	Q6VAB6	950	107.6	Kinase suppressor of RAS 2; dimerizes with BRAF and promotes BRAF-mediated phosphorylation of MEK1 and MEK2
ERK1	P27361	379	43.1	*E*xtracellular signal-*R*elated protein *K*inase 1; mitogen-activated protein kinase 3 corresponding to the *MAPK3* gene
ERK2	P28482	360	41.4	Mitogen-activated protein kinase 1 corresponding to the *MAPK1* gene

000), endometrial carcinoma (10,000), multiple myeloma (5500), and breast cancer (3600). These data indicate that *KRAS* is the most frequently mutated of the three RAS isoforms in 19 of the 29 cancer types and is responsible for about 85% of *RAS*-mutant cancers. *NRAS* (17% of patients) and *HRAS* (7%) mutations show strong coupling to a smaller subset of cancer types. There are numerous activating codon 12, 13, or 61 mutations that occur in each RAS isoform resulting from a single DNA base change. However, five mutations (G12D, G12V, G12C, G13D, and Q61R) account for 70% of all *RAS*-mutations found in patients. $KRAS^{G12C}$ mutations are the most common mutation in cigarette smokers with lung cancer owing to G:C > T:A transversions associated with bulky adducts generated by the mutagens in tobacco smoke [43]. In contrast, $KRAS^{G12D}$ is the most common mutation observed in lung cancer patients who are nonsmokers.

The spectrum of *RAS* mutations varies with the specific tumor types [44]. For example, *KRAS* mutations are found in nearly 100% of pancreatic ductal adenocarcinomas, about 45% of colorectal carcinomas, and about 30% of lung cancers. The estimated incidence of these malignancies in the United States in 2021 for pancreas is 60,000; lung, 236,000; and colorectum, 150,000 [45]. On the other hand, mutations

Table 2
Classes of PI 3-kinases.[a]

PI3K classes	Catalytic subunits (*gene*) tissue distribution	Regulatory subunits (*gene*)
Class I		
IA	p110α (*PIK3CA*) ubiquitous p110β (*PIK3CB*) ubiquitous p110δ (*PIK3CD*) hematopoietic	p85α (*PIK3R1*) p55α (*PIK3R1*) p50α (*PIK3R1*) p85β (*PIK3R2*) p55γ (*PIK3R3*)
IB	p110γ (*PIK3CG*) hematopoietic	p101 (*PIK3R5*) p84 (*PIK3R6*)
Class II		
II	PI3KC2α (*PIK3C2A*) ubiquitous PI3KC2β (*PIK3C2B*) ubiquitous PI3KC2γ (*PIK3C2G*) gastrointestinal tract and liver	None
Class III		
Complex I	VPS34 (*PIK3C3*) ubiquitous	Beclin I (*BECN1*) PIK3R4 (*PIK3R4*) ATG14 (*ATG14*)
Complex II	VPS34 (*PIK3C3*) ubiquitous	Beclin I (*BECN1*) PIK3R4 (*PIK3R4*) UVRAG (*UVRAG*)

[a] Data from Ref. [36].

in *HRAS* and *NRAS* rarely occur in these tumors. Both *NRAS* and *KRAS* mutations occur in just about equal frequencies (20% and 23%) in multiple myeloma [44] with an annual incidence of 35,000 in the United States [45]. In contrast, *NRAS* mutations predominate in melanoma (28% vs. 1% in *HRAS* and 0.8% in *KRAS*) with an annual incidence of about 106,000 in the United States. Additionally, codon mutations vary with each RAS isoform [44]. *KRAS* mutations occur predominantly at codon 12 (82%) and *NRAS* mutations occur predominantly at codon 61 (62%) as illustrated in Table 4. On the other hand, activating mutations in *HRAS* are distributed among all three codons: 12 (27%), 13 (25%), and 61 (40%).

Mutations involving the PI3-kinase pathway are among the more common mutations contributing to the pathogenesis of cancer [24,25]. For example, *PIK3CA* encodes the p110α catalytic subunit and it is mutated in greater than 10% of all cancers [46]. This isoform is chiefly responsible for mediating signaling by receptor protein-tyrosine kinases, making p110α an attractive therapeutic target. Furthermore, Zhang et al. reported that *PIK3CA* was amplified in 6% of all cancers [47]. These investigators also found that *PTEN* (phosphatase and tensin homolog) mutations occurred in 9% of all cancers in their data base. The gene product catalyzes the hydrolysis of PIP3 to form phosphatidylinositol 4,5-bisphosphate to thereby reverse the action of PI3-kinase. PI3-kinase overexpression and mutations that increase enzyme activity promote cell growth and proliferation and result in neoplastic transformation. Mutations of *PIK3CA*, *PIK3R1*, *PTEN* are mutually exclusive, but they occur in about one-third of all solid tumors. Besides the high incidence of cancers with mutations involving components of the PI3-kinase pathway, increased PI3-kinase activity results from other driver oncogenic mutations including those of *RAS* [4,28,29] and *ERBB2/HER2* [48–50].

3. The structure of the RAS proteins

The HRAS, KRAS4a, and NRAS encoded polypeptides contain 189 amino acids and that of KRAS4b contains 188 residues (Fig. 3A). The G-domain of each is made up of residues 1–166 and the C-terminal hypervariable domain extends from residue 167 to residues 188/189. The G-domain consists of six β-strands that are surrounded by five α-helices (Fig. 3B/C). The primary structure of the catalytic domains of the RAS isoforms is highly conserved; residues 1–86 are invariant among the four RAS proteins and make up the effector lobe. This region includes residues that are critical for RAS functioning including switch I (S-I; residues 30–40) and switch II (S-II; residues 58–72), which engage effectors [51]. The switch residues interact with effector proteins such as RAF and PI3K as well as the regulatory GEFs and GAPs. The P-loop, or phosphate loop, that is adjacent to the GTP phosphates is made up of residues 10–14. The mutation hotspots in cancer are in the P-loop (G12/13) or in switch II (Q61). Residues 87–172 make up the allosteric lobe, which exhibits about 86% identity across the RAS isoforms. Each RAS isoform ends with a CaaX box sequence where C is cysteine, a is any aliphatic residue, and X is serine or methionine. The allosteric lobe and the hypervariable region interact with membranes and contain all the isoform specific differences.

There are three main aspects of RAS structures to consider: (i) their mode of interaction with guanine nucleotides, (ii) their interaction with RAS regulators and effectors, and (iii) their interaction with drugs. Although the initial structural studies focused in HRAS, we will consider later work with KRAS – when available – owing to the preponderance of *KRAS* mutations in cancer. Active RAS contains GTP while inactive RAS

Table 3
PI3-kinase pathway components.

Component	UniprotKB no.	No. of amino acids	MW (kDa)	Comments
Lipid kinases				
PI3Kα	P42336	1068	124.3	PI3-kinase α; upstream of PDK1 & AKT in the PI3K pathway
PI3Kβ	P42338	1070	122.8	PI3-kinase β; upstream of PDK1 & AKT
PI3Kδ	O00329	1044	119.5	PI3-kinase δ; upstream of PDK1 & AKT
PI3Kγ	P48736	1102	119.5	PI3-kinase γ; upstream of PDK1 & AKT
PI3K-C2α	O00443	1686	190.7	Phosphatidylinositol 4-phosphate 3-kinase C2 domain-containing subunit alpha; upstream of AKT
PI3K-C2β	O00750	1634	184.8	Phosphatidylinositol 4-phosphate 3-kinase C2 domain-containing subunit beta; involved in EGFR and PDGFR signaling and upstream of AKT
PI3K-C2γ	O75747	1445	165.7	Phosphatidylinositol 4-phosphate 3-kinase C2 domain-containing subunit gamma; upstream of AKT
Protein kinases				
PDK1	O15530	556	63.1	3-*P*hosphoinositide-*D*ependent protein *K*inase 1; mediates the phosphorylation of many protein kinases including AKT1/2/3 and plays a role in many signal transduction pathways
AKT1	P31749	480	55.7	RAC-α serine/threonine-protein kinase with hundreds of substrates and diverse functions including cell survival
AKT2	P31751	481	55.8	RAC-β serine/threonine-protein kinase with diverse functions including insulin signaling
ATK3	Q9Y243	479	55.8	RAC-γ serine/threonine-protein kinase expressed chiefly in brain
mTOR	P42345	2549	288.9	Mammalian target of rapamycin protein-serine/threonine kinase with as many as 800 substrates; makes up mTORC1/2 signaling complexes that participate in cell growth, proliferation, survival, and protein synthesis

Table 4
RAS mutation frequency.[a]

Allele	Codon 12	Codon 13	Codon 61	Sum of columns 2–4[b]
KRAS, 15.8% of all cancers	82% G12D (33.65%) G12V (23.0%) G12C (11.4%)	14% G13D (12.6%) G13C (0.8%) G13S (0.2%)	2% Q61H (1.3%) Q61R (0.4%) Q61L (0.3%)	98%
NRAS, 2.4%	23% G12D (12.4%) G12S (3.9%) G12C (2.7%)	11% G13D (5.9%) G13R (2.6%) G13V (1.5%)	62% Q61R (29.0%) Q61K (21.9%) Q61L (6.3%)	96%
HRAS, 0.7%	27% G12V (13.3%) G12S (5.3%) G12D (4.7%)	25% G13R (19.3%) G13D (1.8%) G13V (1.8%)	40% Q61R (18.6%) Q61L (10.5%) Q61K (8.2%)	92%

[a] Data from Ref. [44].
[b] Not 100% due to rounding errors, approximations, and other mutations not listed.

contains GDP and differences in their structures should help to explain their dissimilar properties. The early work of Milburn et al. indicated that the chief variation of the active and inactive forms of RAS (HRAS in their studies) resided in the switch I and switch II regions, which they defined and named [52]. Both regions are highly exposed and occur on the molecular surface of HRAS, KRAS, and NRAS where they can interact with regulatory and effector molecules. The functional differences are related to the presence (GTP) or absence (GDP) of the γ-phosphate of the guanine nucleotide. In the GTP state, the γ-phosphate forms polar bonds with T35 in switch I and G60 in switch II (Fig. 4A).

Except for the γ-phosphate, the interactions of the guanine nucleotide and RAS are similar in the GDP and GTP states [52]. The guanine base interacts with the side chains of N116, D119, and the backbone of A146. The ribose of GDP and GTP interacts with the backbone of D30 and K117. The α-phosphates interact with the backbones of G15 and A18 and the β-phosphates interact with the backbones of G13, V14, K16, and S17. The Mg^{2+} ion coordinates with the sidechain (GDP state) or the backbone (GTP state) of S17 and the β-phosphate (GDP state) or β- and γ-phosphate (GTP state) (Fig. 4B/C). The γ-phosphate interacts with S17, T35, and G60. The interaction of the γ-phosphate with T35 and G60 is strained in the GTP active-RAS state and these residues shift to an extended and relaxed position in the GDP inactive-RAS state (Fig. 4A). In contrast, the S17 residues are superimposable in both states (not shown). The strained and relaxed structures represent the two states of the RAS proteins.

Milburn et al. hypothesized that the switch I and switch II regions that occur on the surface of the RAS proteins are important in their interaction with regulators and effectors [52]. Subsequent studies have demonstrated that this idea is correct. Numerous switch I and switch II residues of KRAS interact with the RAS-binding domain of NF1 (Fig. 5A). E33, E37, D38, and S39 (all switch I) form hydrogen bonds with N1430, K1419, K1423, and E1437, respectively. Similarly, Q61, E62, E63, and Y64 (all switch II) form hydrogen bonds with G1277, N1278, T1286, and L1390. E37 and D38 (both switch I) form salt bridges with K1419 and K1423 while E62 and E63 (both switch II) form ionic bonds with K1283 and R1391. Of the 20 residues from KRAS that interact with NF1, nine are derived from switch I and eight are derived from switch II.

Rabara et al. determined the X-ray crystal structure of KRAS-GMPPNP (5′ guanylyl-imidodiphosphate) bound to a portion of neurofibromin-1 [53]. Residues in the GTPase active site include KRAS Q61, Mg^{2+} bound to KRAS T35, and NF1 R1276 (the arginine finger) (Fig. 6). One of the functions of positively charged R1276 is to neutralize the negative charge of the phosphate group. These investigators suggest that a hydrogen bond forms between the amide nitrogen of the KRAS Q61 side chain and the main-chain carbonyl oxygen of the arginine finger (not evident in this conformation). These changes in the active site are postulated to stabilize and orient KRAS Q61 and NF1-R1276 in the active site for the GTP hydrolysis reaction. Q61 is a highly conserved residue that may activate a water molecule for an inline nucleophilic attack on the γ-phosphate of GTP [54].

Analysis of the interaction of KRAS with SOS1 indicates that E31, Y32, and R41 (all switch I) form polar bonds with K963, N944, and D910 of SOS1, respectively. A59, G60, E63, S65, D69, Q70, and Y71 (all switch II) form polar bonds with T935, W809, R826, E1002, S881, S908, and Y912. E63 forms a second polar bond with K814. Of the 31 KRAS residues at the KRAS-SOS1 interface, six are furnished by switch I and eleven by switch II (Fig. 5B). Thus, only about one-half of this interface is comprised of switch residues. A study of the KRAS-CRAF interface indicates that four switch I residues form polar bonds with six CRAF residues: E31-K84, D33-K84, E37 with R59 and R67, D38 with T68 and R89, respectively. Of the 12 KRAS residues at this interface, eight belong to switch I and one belongs to switch II (Fig. 5C). Examination of the HRAS–PI3-kinase interface shows that D33 (switch I) forms polar bonds with K251 and K255; moreover, S39 (also switch I) forms hydrogen bonds with S230. Additionally, E37 (switch II) forms hydrogen bonds with T232 and a hydrogen bond and salt bridge with K223. Of the 11 interface residues in this complex, five belong to switch I and one is from switch II (Fig. 5D). These data indicate that there is variation in the KRAS effector residues from case to case, but the end result is that the switch residues are an important participant in these interactions.

4. Development of KRAS inhibitors

Although the RAS oncogenes were among the first oncogenes to be discovered, three decades of effort were required to identify potentially efficacious RAS protein inhibitors for clinical use. Oncogenic *RAS* mutations produce the functional activation of this family of proteins by diminishing GTP hydrolysis [55]. The RAS isoforms bind to GDP and GTP with picomolar affinity, which makes it very difficult to develop guanine nucleotide-competitive inhibitors. Furthermore, the RAS proteins lack other deep surface pockets thereby hindering efforts to identify high-affinity antagonists. This combination of protein properties led to the notion that RAS isoforms are undruggable proteins.

In a pioneering study published in 2013, Shokat et al. developed covalent inhibitors that targeted the reactive C12 of mutant $KRAS^{G12C}$ [55]. They hypothesized that covalent modification of this residue would allow for the continual inhibition of $KRAS^{G12C}$-driven signaling by allowing relatively low affinity, noncovalent attraction to the protein to be followed by the formation of an irreversible covalent bond resulting in the permanent inactivation of the oncogenic driver. This strategy targets the mutant protein with the potential to minimize adverse toxic events by leaving the wildtype protein unmodified. Given the long protein half-life of KRAS (≈ 22 h), covalent inactivation allows for a durable pharmacodynamic response [56]. The mutant C12 residue is near the GTP/GDP pocket and the switch regions that participate in effector interactions. Shokat et al. screened a library of compounds with the potential to form disulfide cross links with the mutant protein. Their early lead compounds failed to modify the three native HRAS cysteine residues and reacted only with C12. Moreover, the reaction was not diminished by 1 mM GDP indicating that their compounds modify an allosteric site that does not overlap with GDP. In contrast, the GTP-state of $KRAS^{G12C}$ exhibits diminished reactivity with their thiol reagents indicating incompatibility between compound binding and the active

(A) RAS primary structures

```
HRAS     10        20        30        40        50        60        70
MTEYKLVVVG AGGVGKSALT IQLIQNHFVD EYDPTIEDSY RKQVVIDGET CLLDILDTAG QEEYSAMRDQ
         80        90        100       110       120       130       140
YMRTGEGFLC VFAINNTKSF EDIHHYREQI KRVKDSEDVP MVLVGNKCDL PSRTVDTKQA QDLARSYGIP
        150       160       170       180
YIETSAKTRQ GVEDAFYTLV REIRQHKLRK LNPPDESGPG CMSCKCVLS

KRAS4a   10        20        30        40        50        60        70
MTEYKLVVVG AGGVGKSALT IQLIQNHFVD EYDPTIEDSY RKQVVIDGET CLLDILDTAG QEEYSAMRDQ
         80        90        100       110       120       130       140
YMRTGEGFLC VFAINNTKSF EDIHHYREQI KRVKDSEDVP MVLVGNKCDL PSRTVDTKQA QDLARSYGIP
        150       160       170       180
FIETSAKTRQ RVEDAFYTLV REIRQYRLKK ISKEEKTPGC VKIKKCIIM

KRAS4b   10        20        30        40        50        60        70
MTEYKLVVVG AGGVGKSALT IQLIQNHFVD EYDPTIEDSY RKQVVIDGET CLLDILDTAG QEEYSAMRDQ
         80        90        100       110       120       130       140
YMRTGEGFLC VFAINNTKSF EDIHQYREQI KRVKDSDDVP MVLVGNKCDL AARTVESRQA QDLARSYGIP
        150       160       170       180
FIETSAKTRQ GVDDAFYTLV REIRKHKEKM SKDGKKKKKK SKTKCVIM

NRAS     10        20        30        40        50        60        70
MTEYKLVVVG AGGVGKSALT IQLIQNHFVD EYDPTIEDSY RKQVVIDGET CLLDILDTAG QEEYSAMRDQ
         80        90        100       110       120       130       140
YMRTGEGFLC VFAINNSKSF ADINLYREQI KRVKDSDDVP MVLVGNKCDL PTRTVDTKQA HELAKSYGIP
       150       160       170       180
FIETSAKTRQ GVEDAFYTLV REIRQYRMKK LNSSDDGTQG CMGLPCVVM
```

(B) RAS secondary structure

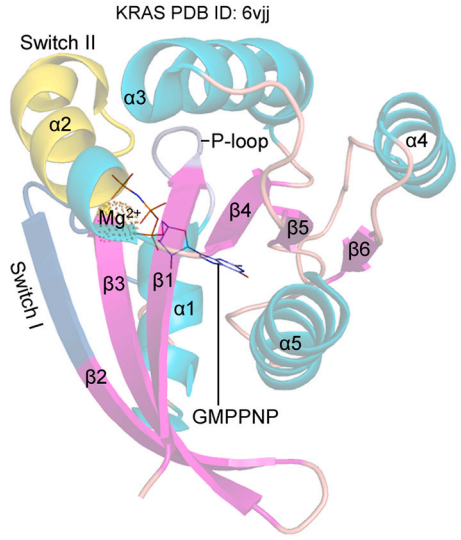

(C) RAS secondary structure

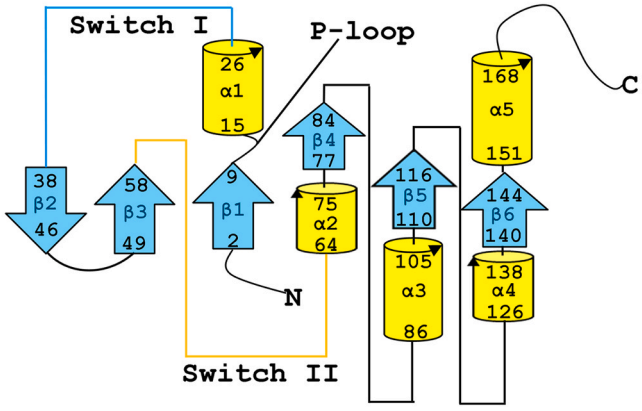

Fig. 3. (A) Primary structures of the human RAS proteins. The phosphate loop residues are highlighted in cyan; switch II residues, yellow; switch I residues are colored blue; and the hypervariable residues are colored red. (B) RAS structure. (C) RAS secondary structure. α-Helices are shown as yellow cylinders and β-sheets, blue arrows. The numbers indicate the beginning and end of each segment. N denotes the amino terminus and C denotes the carboxyterminus.

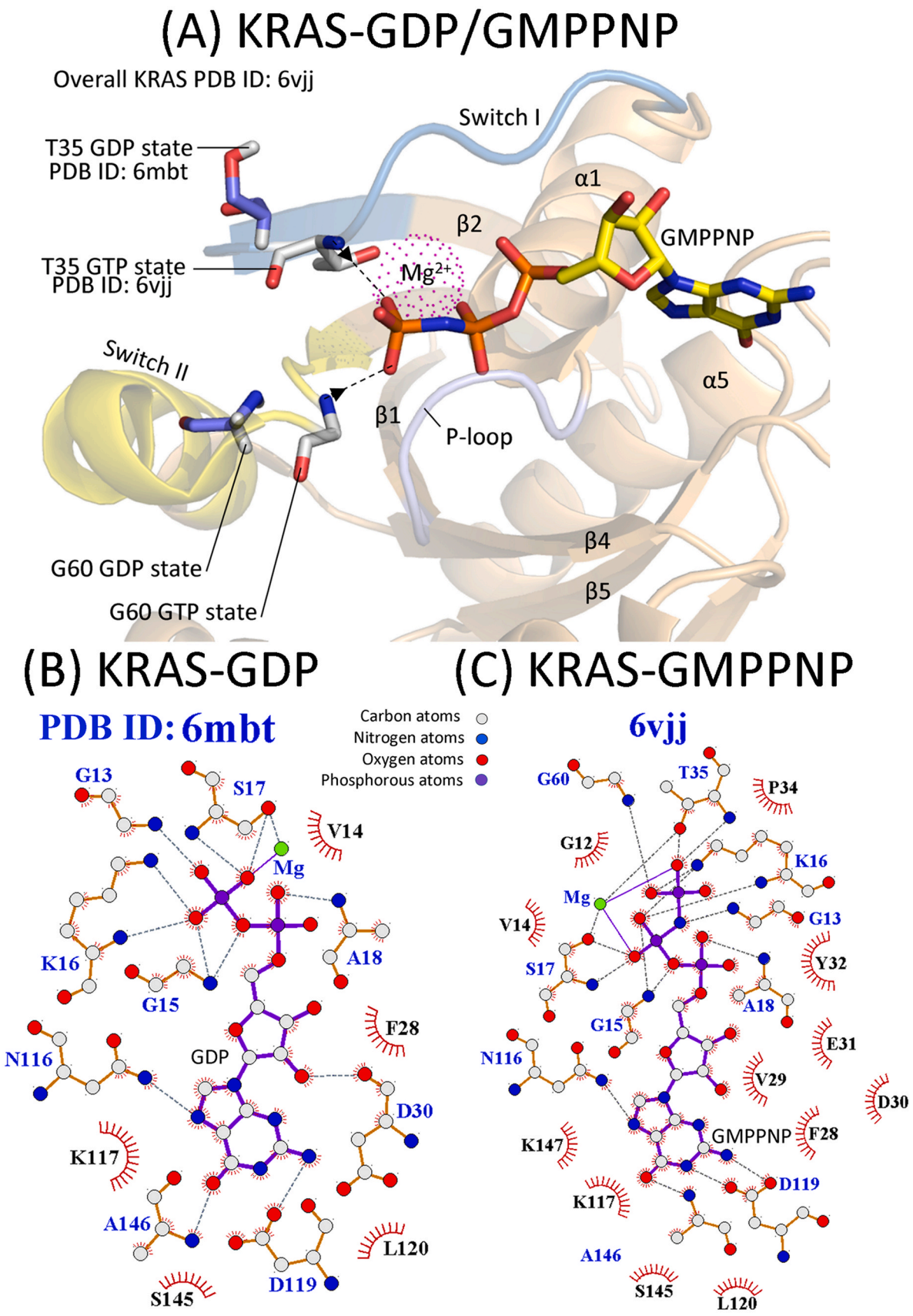

Fig. 4. (A) Superposition of the GDP and GTP states of KRAS. T35 and G60 are tightly linked to the γ-phosphate, but they are in a distant relaxed conformation in the RAS-GDP state. (B) Interaction of GDP with KRAS. (C) Interaction of GMPPNP with KRAS. Dashed lines in 4B and 4C denote polar bonds and the sun rays signify non-bonded interactions as calculated by LIGPLOT v.4.5.3 (https://www.ebi.ac.uk/thornton-srv/software/LIGPLOT/).

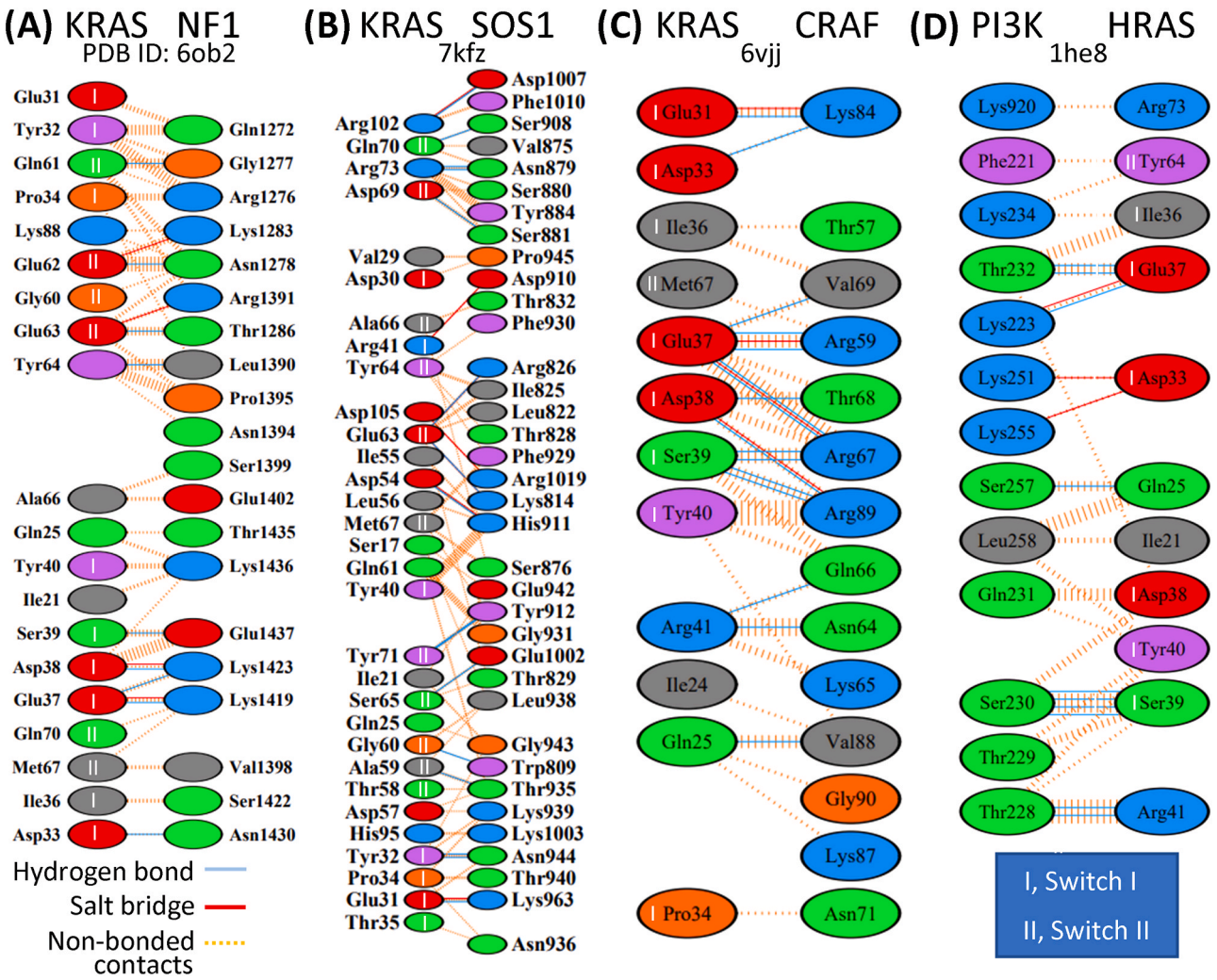

Fig. 5. RAS protein-protein hydrogen bond, salt bridge, and non-bonded contacts. The schematic representation of the four RAS interaction interfaces was created by PDBSum (http://www.ebi.ac.uk/thornton-srv/databases/cgi-bin/pdbsum/GetPage.pl?pdbcode=index.html). The interactions are indicated by the following notation: hydrogen bonds, blue solid lines; salt bridge, red solid lines; non-bonded contacts, striped lines (width of the striped line is proportional to the number of atomic contacts). I labels the RAS switch I residues; II, switch II residues.

conformation of RAS.

Ostrem et al. focused on the reactivity of compound **6** (Fig. 7A) with a $KRAS^{G12C}$ construct that lacked the three native cysteines (C51S/C80L/C118S) in order to eliminate the possibility of any adventitious reactions of the chemical warhead with the KRAS construct; the X-ray crystal structure of this construct was essentially the same as that of mutant $KRAS^{G12C}$ [55]. They confirmed that compound **6** does not bind in the GDP pocket, but extends from C12 into an adjacent pocket composed largely of switch II as well as other residues (Fig. 8A). The covalently linked compound **6** forms a hydrogen bond with G60 (Fig. 8B). The interaction of the ligand is illustrated in Fig. 8C where the interacting residues are shown as spheres where the yellow residues are made up of switch II components and the light blue spheres are additional residues that make up the pocket. These investigators called this the switch II pocket (S-IIP). This fully formed pocket is not apparent in native RAS structures. The residues that make up this pocket are listed in Table 5. S-IIP is located between the central β-sheet of RAS and the α2- and α3-helices. Whereas the switch-II residues are re-ordered to produce the pocket, the switch-I residues have the same disposition as that observed in the KRAS GDP-bound state. The discovery of the switch-II pocket paved the way to the discovery of other $KRAS^{G12C}$ inhibitors as described next.

Lanman et al. provided a comprehensive description on the development of an indole compound (Fig. 7B) that led to the formulation of sotorasib, a substituted pyrido[2,3-*d*]pyrimidin-2-one (Fig. 7C) bearing an acrylamide warhead that is attacked by the mutant C12 thiol group of $KRAS^{G12C}$ [56]. Structural studies with their lead compound demonstrated that it occupied a previously unknown cryptic pocket on the surface of KRAS that was made up of H95, Y96, and Q99 and they exploited this pocket during the design of sotorasib. The X-ray crystal structure shows that the drug makes numerous contacts with the switch II-pocket residues that are portrayed in Fig. 8D. Moreover, it forms polar bonds with the carbonyl group of E63 and the side chains of R68 and K16 (Fig. 8E). Sotorasib fits snugly into the switch II pocket as depicted in Fig. 8F, which also shows the location of the residues that make up the cryptic pocket that contain the methylisopropylpyridine group. Several of the properties of the drug are listed in Table 6. With the exception of a molecular weight of 560, this drug falls within the guidelines of Lipinski's rule of five (Ro5) for orally bioavailable drugs. The Ro5 implies that less than ideal oral effectiveness is more likely to be found when (i) the calculated Log P (cLogP) is more than 5, when (ii) there are more than 5 hydrogen-bond donors, when (iii) there are more than 5 × 2 or 10 hydrogen-bond acceptors, and when (iv) the molecular weight is more than 5 × 100 or 500 [57]. The partition coefficient (P) is the ratio of the solubility of the un-ionized drug in the organic phase of water-saturated *n*-octanol divided by its solubility in the aqueous phase

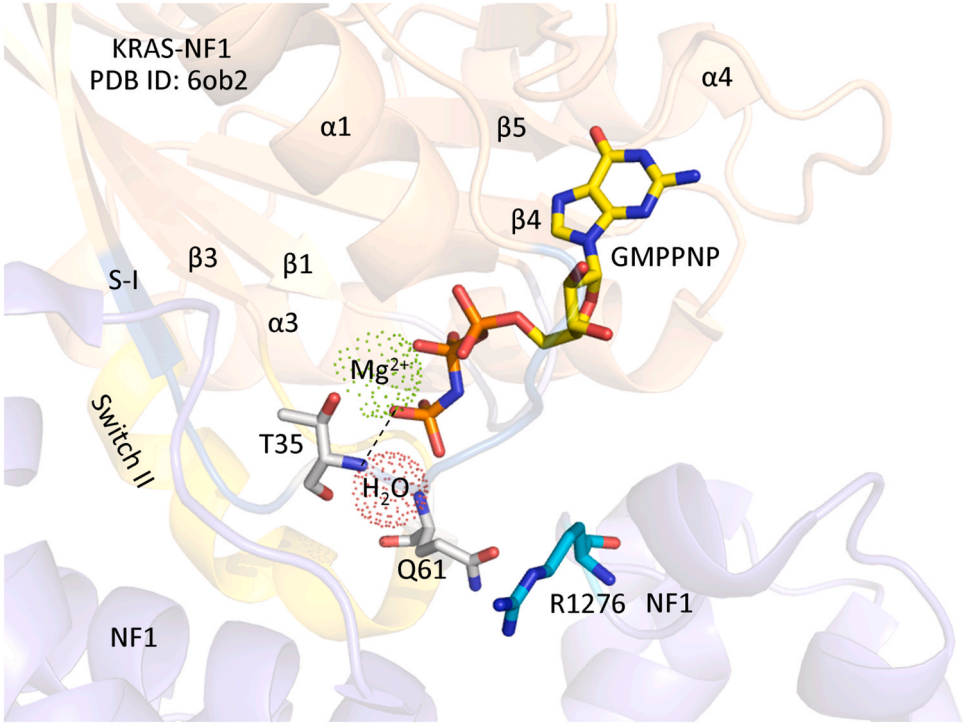

Fig. 6. The GTPase active site of the KRAS-NF1 GAP complex. The arginine finger (R1276) from NF1 is inserted into the active site of KRAS and is a necessary participate in the stimulation of GTPase activity. S-I, switch I.

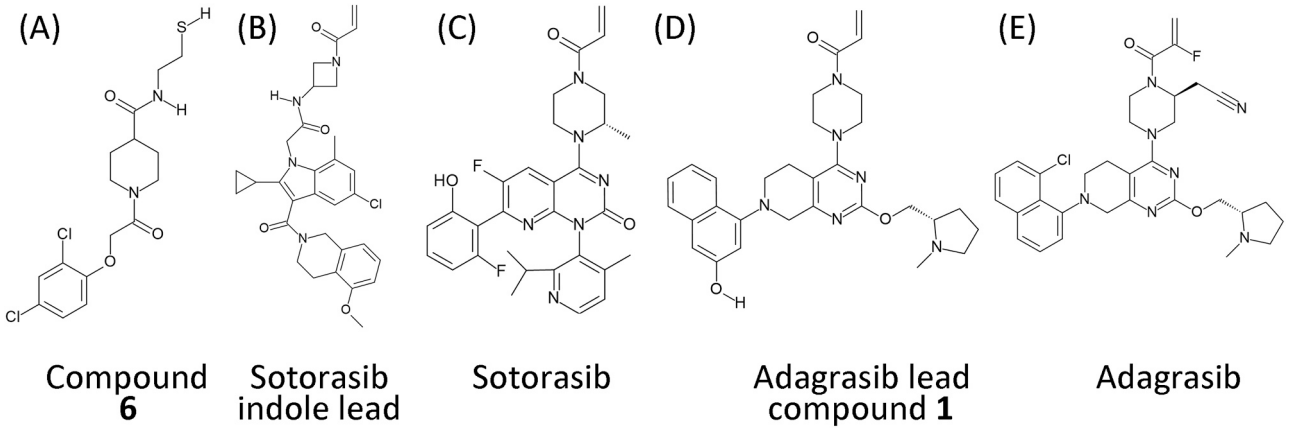

Fig. 7. Structures of selected KRAS^{G12C} covalent inhibitors and their lead compounds.

and is a measure of hydrophobicity.

Sotorasib is a targeted covalent inhibitor (TCI) of KRAS^{G12C} that is FDA-approved for the second-line treatment of adult patients with *KRAS^{G12C}*-mutated metastatic or locally advanced non-small cell lung cancer (NSCLC), as determined by an FDA-approved test, and it is approved for patients who have received at least one prior systemic therapy. Sotorasib is currently in six clinical trials for various advanced solid tumors including NSCLC both alone and in combination with immunotherapies, cytotoxic therapies, and targeted therapies (ClinicalTrials.gov). This drug demonstrated encouraging anticancer activity in patients with heavily pretreated advanced, or metastatic, solid tumors bearing the *KRAS^{G12C}* mutation. Of 126 patients with advanced NSCLC, a total of 46 experienced an objective response (four with a complete response and 42 with a partial response) with an overall response rate of 37% and a disease control rate of 80% [58,59]. The median time to an objective response was 1.4 months and the median duration of the response was 11.1 months with a median progression free survival of 6.8 months. Adverse events of any grade, regardless of attribution, were observed in 125 patients (99.2%); the most common adverse events were diarrhea (in 64 patients or 50.8%), nausea (in 39 or 31.0%), fatigue (in 32 or 25.4%), arthralgia (in 27 or 21.4%), an increase in the aspartate aminotransferase (in 27 or 21.4%), and an increase in the alanine aminotransferase (in 26 or 20.6%). There were no treatment-related deaths. In a study with 42 patients with *KRAS^{G12C}*-mutation–positive colorectal cancer, only 7% had a confirmed response and 74% had disease control [58]. See Refs. [58–60] for summaries of the findings of sotorasib (Lumakras) clinical trials.

Although sotorasib is the only FDA-approved KRAS^{G12C} inhibitor, adagrasib (MRTX849) is a promising agent that is also a targeted covalent inhibitor. Beginning with a tetrahydropyridopyrimidine lead compound (Fig. 7D), Fell et al. described the numerous steps in the formulation of adagrasib [61]. The presence of a hydroxyl group on the lead compound promoted its metabolism to glucuronides so that the deshydroxy analog was generated for further development. These

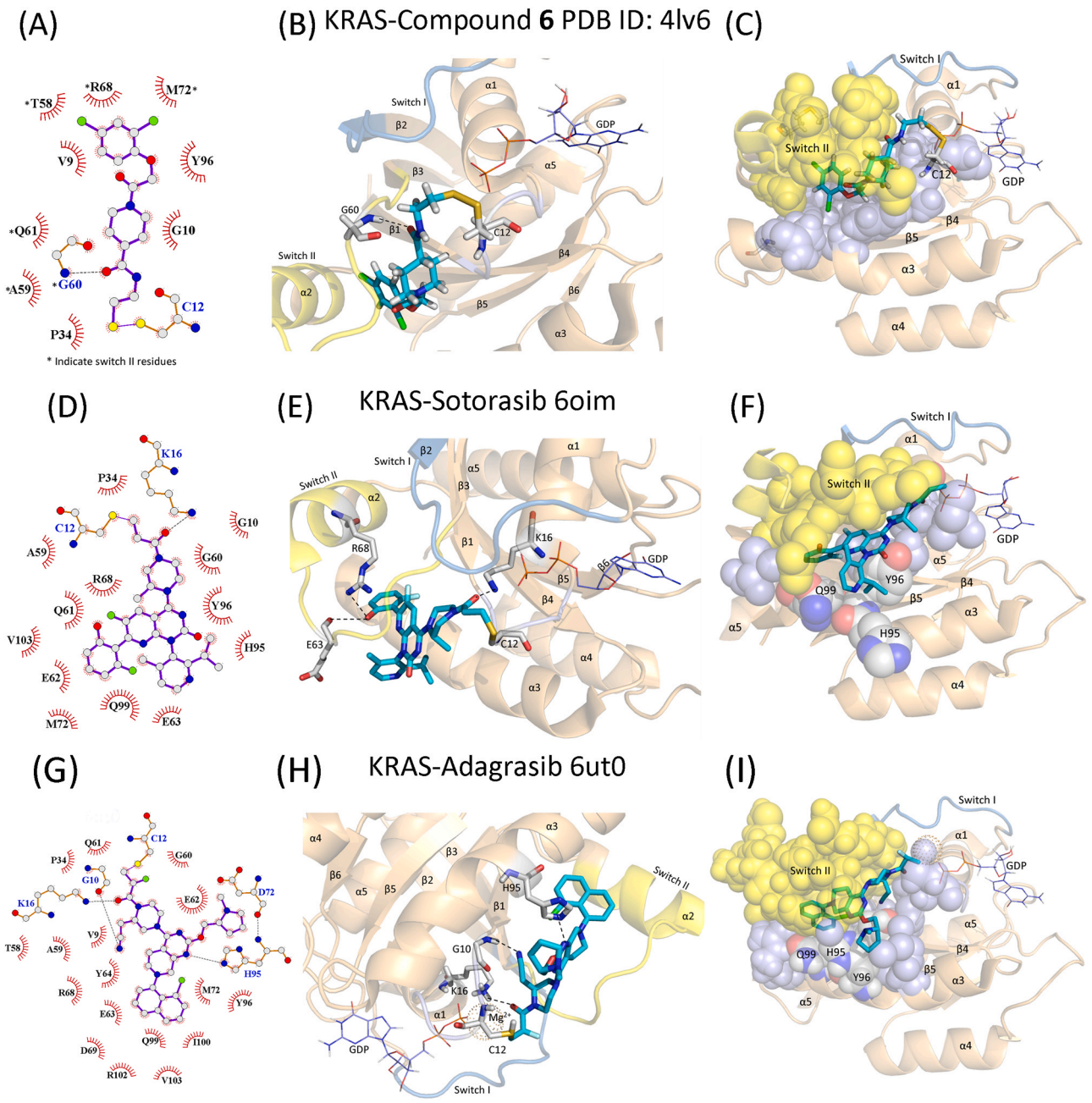

Fig. 8. (A) Interaction of compound **6** with KRAS as calculated by LIGPLOT v.4.5.3. (B) Compound **6** forms a single hydrogen bond with KRAS G60. (C) Interaction of compound **6** with the switch II pocket as depicted in spheres. The yellow residues are S-II components and the light blue residues are additional residues that make up the switch II pocket. (D) Interaction of sotorasib with KRAS; only one of three polar bonds is shown. (E) Sotorasib forms a hydrogen bond with each of three KRAS residues (K16, E63, R68) and a covalent bond with C12. (F) Interaction of sotorasib with the switch II pocket as depicted in spheres. (G) Interaction of adagrasib with KRAS. (H) Adagrasib forms a hydrogen bonds with each of three KRAS residues (G10, K16, H95) and a covalent bond with C12. (I) Interaction of adagrasib with the switch II pocket as depicted in spheres.

Table 5
List of all residues of the switch II pocket.[a]

V9	T35 (S-I)	E63 (S-II)	F78	I100
G10	A59 (S-II)	Y64 (S-II)	D92	R102
C12	G60 (S-II)	R68 (S-II)	H95	V103
K16	Q61 (S-II)	D69 (S-II)	Y96	
P34 (S-I)	E62 (S-II)	M72 (S-II)	Q99	

[a] S-I and S-II denote members of the switch I and switch II regions of RAS [51], respectively.

investigators used X-ray crystal structures to formulate a strategy for implementing molecular changes in their inhibitory compounds. Accordingly, piperazine derivatives were introduced to displace a water bound to the side chain of T58 and the carbonyl group of G10. This strategy is designed to increase the affinity of the drug for its target. Addition of a cyanomethyl group to the piperazine increased the potency of an intermediate drug by 300-fold. Moreover, these investigators attached a chlorine atom to the naphthyl ring to produce a derivative that filled a lipophilic KRAS drug pocket made up of V9, T58, M72, and Y96. The end product of this process (adagrasib) is illustrated in Fig. 7E.

Several properties of adagrasib are listed in Table 6. The properties fall within the criteria of Lipinski's Ro5 for an orally effective drug with

Table 6
Properties of selected $KRAS^{G12C}$ inhibitors.[a]

Drug	PubChem CID	Formula	MW (Da)	HD[b]	HA[c]	cLogP[d]	Rotatable bonds	PSA[e] (Å^2)	Ring count	Complexity[a]
Compound **6**	71815953	$C_{16}H_{20Cl2}N_2O_3S$	391	2	4	2.9	6	59.6	2	434
Sotorasib	137278711	$C_{30}H_{30}F_2N_6O_3$	561	1	7	4.0	5	102	5	1030
Adagrasib	138611145	$C_{32}H_{35}ClFN_7O_6$	604	0	9	4.2	7	88.8	6	1060

[a] Data from NIH PubChem (https://pubchem.ncbi.nlm.nih.gov/) except for cLogP.
[b] No. of hydrogen bond donors.
[c] No. of hydrogen bond acceptors.
[d] Calculated Log_{10} of the partition coefficient was computed using MedChem DesignerTM, version 2.0, Simulationsplus, Inc. Lancaster, CA 93534.
[e] PSA, Polar Surface Area.

the exception of the molecular weight of 604 Da [57]. Data from the X-ray crystal structure of adagrasib bound to $KRAS^{G12C}$ demonstrates that there is extensive interaction with residues of the switch II pocket (Fig. 8G). Furthermore, there are polar bonds of the drug with G10, the ε-amino group of K16, and the NE2 nitrogen of H95 (Fig. 8H). Adagrasib makes hydrophobic contact with V9, K16 and switch II residues T58, A59, Q61, E62, Y64, R68, and M72. It also makes hydrophobic contact with Y96, Q99, I100, and V103. Note that H95, Y96, and Q99 do not form a cryptic pocket that interacts with this drug as observed for sotorasib. Adagrasib fits snugly into the switch II pocket as depicted in Fig. 8I.

This drug is currently in five clinical trials for various solid tumors including NSCLC and colorectal cancer alone and in combination with immunotherapies, cytotoxic therapies, and targeted therapies (ClinicalTrials.gov). Among 51 patients with $KRAS^{G12C}$-mutation–positive NSCLC who had progressed after standard treatments, the objective response rate was 45% and the disease control rate was 96% [60]. The drug had a manageable safety profile. The most common grade 3 or greater treatment adverse events included nausea, vomiting, diarrhea, fatigue, and elevated aminotransferase levels and these are the same as described for sotorasib, perhaps indicating that these are drug class effects.

Acquired resistance to cytotoxic, immune, and targeted therapies in patients with advanced cancers is nearly universal and that resistance occurs in patients with the $KRAS^{G12C}$ mutation that were treated with sotorasib or adagrasib is not surprising. Awad et al. studied the adagrasib resistance mechanisms of a cohort of 38 patients including 27 with NSCLC, 10 with colorectal cancer, and one with appendiceal cancer [62]. Resistance mechanisms were found in 17 patients of whom 7 exhibited multiple coincident mechanisms. Several had new *KRAS* mutations including G12D (1 with NSCLC and 3 with CRC), G12R (1 CRC), G12V (1 NSCLC/1 CRC), G12W (1 NSCLC), G13D (3 CRC), Q61H (1 CRC), H95D (1 NSCLC), H95Q (1 CRC), H95R (2 CRC), and Y96C (1 NSCLC). Several had acquired bypass mechanisms including MET amplification (2 NSCLC) and *NRAS* (1 CRC), *BRAF* (1 NSCLC/1 CRC), *MAP2K1* (encoding MEK1, 1 CRC), and *RET* (1 NSCLC) mutations. Several developed oncogenic fusion proteins involving ALK (1 CRC), BRAF (2 CRC), CRAF (2 CRC), FGFR3 (1 CRC), and RET (1 CRC).

It is worth commenting on a few aspects of this study. First, these investigators found that the H95D, H95Q, or H95R mutations, which are insensitive to adagrasib, do not confer resistance to sotorasib in vitro [62]. Second, the samples from patients with colorectal cancer exhibit a greater variety of resistance mechanisms than those from patients with NSCLC. Third, there is a large assortment of adagrasib resistance mechanisms. This contrasts with *EGFR*-mutant lung cancer where resistance to EGFR inhibitors (erlotinib, gefitinib) is predominantly due to the $EGFR^{T790M}$ mutation [49]. This allowed the development of a second-generation inhibitor such as osimertinib that is effective against the initial resistance mechanism [63]. Owing to the variety of resistance mechanisms involving *KRAS* mutations and several bypass pathways, a single antagonist cannot be developed to counteract the resistance to adagrasib. Another notable result of this study is that these investigators were able to elucidate resistance mechanisms in 6 of 10 colorectal cancer patients, but only 10 of 26 NSCLC patients.

5. Approaches to target RAS indirectly

5.1. Inhibitors of RAS post-translational processing

Nucleotide exchange, membrane localization, and effector binding are required for the functioning of RAS [64]. Blocking any of these essential steps will inhibit RAS functioning. RAS requires three enzymatic post-translational processing events to associate with the inner leaflet of the plasma membrane. First, prenylation of the CaaX box at the C-terminal end as catalyzed by farnesyltransferase (FTase) or geranylgeranyltransferase (GGTase-1) is necessary [65]. Second, the cleavage of the aaX residues as catalyzed by RAS-converting enzyme (RCE1) is essential [64]. Third, methylation of the remaining cysteine of the CaaX box as catalyzed by isoprenylcysteine carboxyl methyltransferase (ICMT) is required for membrane association and RAS function [64]. Palmitoylation of HRAS C181, NRAS C181, or KRAS4a C180 as catalyzed by palmitoyltransferase promotes the membrane association of these isoforms [66]. KRAS4b contains a polybasic segment (^{175}KKKKKKSKTK^{184}) that promotes the membrane association of this RAS isoform; it lacks a cysteine residue in the hypervariable region.

Considerable work on FTase inhibitors was performed at the turn of the 21st century, but the clinical results were disappointing [66]. This enzyme prefers methionine or serine at the X position whereas GGTase-1 prefers leucine or isoleucine [67,68]. All RAS isoforms are farnesylated under physiological conditions. However, when cells or patients are treated with FTase inhibitors, KRAS and NRAS, but not HRAS, become geranylgeranylated and are able to interact with the plasma membrane and are fully functional. Accordingly, blockade of FTase is sufficient to inhibit the action of HRAS, but inhibiting both FTase and GGTase-1 is required to block the action of KRAS and NRAS. It appears that there has been a resurgence of interest in the strategy of inhibiting *HRAS* mutants using tipifarnib for the treatment of patients with head and neck squamous cell carcinoma and thyroid cancer and time will tell if this strategy is successful [64].

5.2. Inhibitors of the RAF-MEK-ERK MAP kinase pathway

A/B/CRAF are protein kinases that are activated by the RAS proteins [14,15]. There are five targeted FDA-approved RAF inhibitors: dabrafenib, encorafenib, regorafenib, sorafenib, and vemurafenib. Dabrafenib, encorafenib, and vemurafenib are $BRAF^{V600E}$ inhibitors that were approved for the treatment of melanomas bearing the V600E mutation [69,70]. Coupling MEK1/2 inhibitors with BRAF inhibitors is more effective in treating such melanomas and dual therapy is now the standard of care. Dabrafenib and trametinib, vemurafenib and cobimetinib, and encorafenib plus binimetinib are the FDA-approved combinations for the treatment of $BRAF^{V600E}$ melanomas. Although such mutations occur in other neoplasms including thyroid, colorectal, and NSCLC, these agents are not as effective in treating these nonmelanoma neoplasms. However, dabrafenib is FDA-approved for the treatment of NSCLC and anaplastic thyroid cancers. Additionally, encorafenib is approved for the treatment of colorectal cancer bearing the $BRAF^{V600E}$ mutation. These data indicate that targeted RAF inhibitors have a place

in the armamentarium against specific neoplasms. Regorafenib is a multikinase inhibitor with activity against VEGFR1/2/3, BCR-Abl, BRAF, $BRAF^{V600E}$, Kit, PDGFRα/β, RET, FGFR1/2, Tie2, and Eph2A [71]. It is FDA-approved for the treatment of advanced colorectal cancer and gastrointestinal stromal tumors [71]. The drug is less effective against colorectal cancer bearing *RAS* mutations than against these tumors with wildtype RAS [72]; the nature of the *RAS* mutations in this study was not specified.

Although dabrafenib, encorafenib and vemurafenib are FDA-approved for the treatment of various neoplasms with BRAF mutations, these agents do not work well in *KRAS*-mutant cells [73–75]. Sorafenib is a multikinase inhibitor with activity against B/CRAF, $BRAF^{V600E}$, Kit, Flt3, RET, VEGFR1/2/3, and PDGFRβ [76,77]. It is FDA-approved for the treatment of hepatocellular carcinoma, renal cell carcinoma, and differentiated thyroid cancer [69,70]. Its clinical efficacy in these disorders may be related to its inhibition of angiogenesis and it is in clinical trials in patients with patients bearing *RAS* mutations. However, two clinical studies indicated that sorafenib lacked a noticeable therapeutic effect in people with *KRAS*-mutant NSCLC, the findings of which indicate the inherent resistance to various interventions of tumors bearing *RAS* mutations [75,78]. Moreover, belvarafenib (HM95573) is a RAF antagonist that is in early clinical studies with cobimetinib or with cetuximab (a monoclonal antibody EGFR antagonist) in patients with advanced solid tumors with *RAS* or *RAF* mutations (ClinicalTrials.gov) [75].

Similarly, lifirafenib (BGB-283) is a pan-RAF (A/B/CRAF) inhibitor that is in early clinical trials in patients with solid tumors [79]. Importantly, antitumor activity with prolonged disease control was observed in patients with *KRAS*-mutant cancers, including NSCLC and endometrial carcinoma. In contrast, lifirafenib had limited clinical activity in patients with *KRAS*-mutated colorectal or pancreatic cancers. These results were like those of a phase I clinical trial with RO5126766 (a novel RAF/MEK inhibitor) that showed promise in people with *KRAS*--mutated NSCLC and endometrial/ovarian cancers, but not in patients with *KRAS*-mutated colorectal cancer [79]. Lifirafenib is also in an early clinical trial in combination with the MEK1/2 antagonist mirdametinib in patients with advanced solid tumors (ClinicalTrials.gov).

There are four FDA-approved MEK1/2 protein kinase inhibitors: binimetinib, cobimetinib, selumetinib, and trametinib [70,80]. As noted above, binimetinib, cobimetinib, and trametinib are FDA-approved in combination with BRAF inhibitors for the treatment of melanomas. Trametinib is also FDA-approved for the treatment of patients with $BRAF^{V600E}$-mutation positive NSCLC and selumetinib is approved for the treatment of neurofibromatosis type I (von Recklinghausen disease). Unfortunately, clinical studies indicate that selumetinib (AZD6244, ARRY-142886) or trametinib are ineffective in patients with *KRAS*--mutant NSCLC [81,82]. Martinelli et al. reported that the mechanism for such primary resistance is that MEK1/2 inhibitors have a propensity to promote the paradoxical activation of the MAPK pathway in *KRAS*--mutant tumors [83].

HL-085 is a MEK antagonist (undisclosed structure) that is planned for clinical studies in patients with *KRAS*-mutant positive NSCLC in combination with docetaxel (a drug that inhibits microtubule depolymerization and attenuates the effects of Bcl-2 and Bcl-xL gene expression). Moreover, a clinical trial of binimetinib in combination with erlotinib (an FDA-approved EGFR inhibitor used for the treatment of NSCLC and pancreatic cancer) in patients with NSCLC bearing *KRAS* or *EGFR* mutations is currently underway [75]. A trial of binimetinib in combination with cisplatin and pemetrexed (an antimetabolite) in patients with *KRAS*-mutant NSCLC is also ongoing. Refametinib is a MEK inhibitor that is in clinical studies alone and in combination with (i) sorafenib, (ii) regorafenib, and (iii) copanlisib against various solid tumors including hepatocellular carcinoma (ClinicalTrials.gov). Copanlisib is the PI3-kinase inhibitor mentioned previously. Refametinib had demonstrable activity in patients with *KRAS*-mutant hepatocellular carcinomas [84].

The dual MEK/RAF inhibitor RO5126766 (VS-6766) exhibited antitumor activity in clinical trials in patients harboring *HRAS, KRAS*, *NRAS,* and other mutations in various solid tumors [85]. The subsequent evaluation of RO5126766 in patients with solid tumors or multiple myeloma (12 NSCLC, five with a gynecological malignancy, four with colorectal cancer, one with melanoma, and seven with multiple myeloma) with RAS–RAF–MEK pathway mutations showed that 7 of 26 evaluable patients demonstrated objective responses [86]. Remarkedly, the combination of RO5126766 with defactinib (a focal adhesion protein-tyrosine kinase inhibitor) obtained a 70% overall response rate (7 of 10 evaluable patients) in low grade serous ovarian carcinoma patients harboring *KRAS* mutations [87]. Further clinical studies of RO5126766 for *KRAS*-mutant NSCLC patients are ongoing (NCT03681483 and NCT03875820). The use of a single RAF or MEK inhibitor in the treatment of *KRAS*-driven tumors has demonstrated limited effectiveness. Accordingly, the use of drug combinations represents an alternative strategy. A clinical trial assessing the effectiveness of naporafenib (a BRAF/CRAF inhibitor) with trametinib in patients with *KRAS*- or *BRAF*-mutant NSCLC is underway.

ERK is the final protein kinase in the MAPK pathway [18,19]. The resistance of *KRAS*-mutated tumors to RAF or MEK inhibitors is usually caused by ERK feedback activation of the MAP kinase pathway. Sullivan et al. reported on the findings of an early (phase I) clinical trial on patients with advanced solid tumors using the ERK antagonist ulixertinib [88]. A total of 108 patients was enrolled in six cohorts: patients without prior MAPK-targeted therapy who had *BRAF*-mutant colorectal (17 enrolled/11 evaluable), lung (16/12), or other cancers (24/21), *NRAS*-mutant melanoma (22/18), or any tumor type with a MEK mutation (8/4), and patients with melanoma who had received prior BRAF and/or MEK inhibitor treatment and who were refractory to, intolerant of, or progressed on these treatments (21/15). A variety of specific *BRAF* and *NRAS* mutations were included, as were several different tumor types. Collectively, 91 patients with tumors harboring mutations in *BRAF*, 24 with *NRAS*, 9 with *MEK*, 5 with no mutation identified, and 6 with other mutations (5 *KRAS* and 1 *GNAS*, which encodes a Gα-stimulatory protein) were enrolled. Seventeen patients with *NRAS*-mutated melanoma were evaluable for response. Three patients (18%) achieved a partial response, 6 had stable disease, and 8 had disease progression as the best response. Ulixertinib was generally well tolerated, with manageable and reversible toxicity. The most common side effects included rash (most commonly acneiform), fatigue, and gastrointestinal toxicities, including nausea, vomiting, and diarrhea. Combined inhibition of ERK may be a feasible strategy to prevent drug resistance. A clinical trial is assessing the effectiveness of the ERK1/2 inhibitor LTT462 and trametinib against *NRAS* mutant melanoma (ClinicalTrials.gov). A Phase 1 study of the ERK1/2 inhibitor JSI-1187 administered as monotherapy or in combination with dabrafenib for the treatment of advanced solid tumors with MAPK pathway mutations is also underway.

5.3. Inhibitors of the PI3-kinase pathway

The PI3-kinase-AKT-mTOR pathway is the second major signaling pathway downstream of RAS proteins [25]. There are five FDA-approved PI3-kinase inhibitors: alpelisib, copanlisib, duvelisib, idelalisib, and umbralisib. Alpelisib is an orally effective FDA-approved PI 3-kinase-α inhibitor used for the treatment of breast cancer. Copanlisib, duvelisib, idelalisib, and umbralisib are PI 3-kinase-δ inhibitors that are approved for the third-line treatment of follicular lymphomas and other hematological disorders. Of the five approved drugs, all are orally bioavailable except copanlisib. Each of these agents is in dozens of clinical trials, but none of these studies appear to specifically address the nature of RAS or *RAS* mutations in response to these drugs.

Buparlisib (BKM120) is a class I PI3-kinase inhibitor that is in 89 clinical studies for many tumor types including NSCLC, colorectal, pancreatic, renal cell, breast, prostate cancers, head and neck squamous

cell carcinomas, and other advanced solid tumors (ClinicalTrials.gov). Binimetinib and buparlisib combinations were explored in patients with *KRAS*-, *NRAS*-, or *BRAF*-mutant advanced solid tumors until the maximum tolerated dose and recommended phase II dose were defined [89]. The cohorts were made up of patients with (i) *EGFR*-mutant advanced NSCLC after progression on an EGFR inhibitor, (ii) advanced *RAS*- or *BRAF*-mutant ovarian cancer, or (iii) advanced NSCLC with *KRAS* mutations. Of these cohorts, only six (12%) patients with *RAS*/-*BRAF*-mutant ovarian cancer achieved a partial response. The data indicate that the pharmacokinetics of binimetinib were not altered by buparlisib. Moreover, pharmacodynamic analyses revealed down-regulation of pERK and pS6K in tumor biopsies. Although dual inhibition of MEK and the PI3K pathways showed promising activity in RAS/BRAF ovarian cancer, the overall study with continuous dosing resulted in intolerable toxicities. Alternative scheduling with pulsatile dosing may be advantageous when combining therapies.

Pictilisib (GDC0941) is a class I PI3-kinase inhibitor that is in 17 clinical trials in patients with various solid tumors including those of breast, brain (glioblastoma), and NSCLC. The drug is being evaluated as both a monotherapy as well as in combination with other agents including cobimetinib, erlotinib, palbociclib, and platinum-based cytotoxic agents. It will take considerable effort to tease out the role of mutant *RAS* in the responses to these various mono- and combination therapies. Serabelisib is a PI3-kinase inhibitor that is in ten clinical studies targeting various solid tumors including those of the breast, endometrium, kidney, stomach, and NSCLC. It is being used in combination with everolimus (an mTOR antagonist) and several cytotoxic agents. Considerable effort will be required to address the role of mutant *RAS* in response to these compounds. Inactivation of the MAPK or PI3K pathway alone has poor efficacy in the treatment of *KRAS*-mutated malignancies. The inhibition of the MAPK pathway leads to the activation of the PI3K pathway thereby reducing *KRAS*-mutated cell sensitivity to MEK inhibitors. Accordingly, targeting the P13K-AKT-mTOR and RAF-MEK-ERK pathways simultaneously may be a promising approach. However, this tactic may be limited owing to the potential toxicity associated with this methodology. See Refs. [75,87] for a complete overview of strategies for the treatment of neoplasms with *RAS* mutations.

6. Epilogue

A large percentage of lung adenocarcinomas (32%), pancreatic ductal adenocarcinomas (86%), and colorectal cancers (41%) are driven by *KRAS* mutations [29]. These malignancies represent the three most lethal neoplasms in the United States: cancers of the lung account for 132,000 deaths, those of the colon account for 53,000 deaths, and those of the pancreas account for 48,000 deaths per year [45]. These are followed by breast cancer with 44,000 deaths per year. Despite possessing *KRAS* mutations, NSCLC, colorectal cancer, and pancreatic cancer bear distinct phenotypes with their own tumor microenvironments. Despite some efficacy, these tumors are among the least responsive cancers to immune checkpoint-based therapies [90,91]. A significant number of other cancers are associated with *NRAS* and *HRAS* mutations. Although the RAS proteins have great sequence homology, each RAS protein is a unique entity and must be considered so in the development of direct or indirect inhibitors. In a similar vein, each *KRAS* mutant is unique.

KRAS signaling varies with each tissue and cell type thereby differentially influencing the role of *KRAS* mutations on cancer biology [92]. Specific *KRAS* mutations and expression levels of the mutant KRAS protein vary between various cell types. For example, the $KRAS^{G12C}$ mutation occurs in patients with NSCLC who smoked cigarettes while the $KRAS^{G12D}$ occurs in patients with pancreatic cancer. In these two cases, *KRAS* mutations are a disease-initiating event. In contrast, *KRAS* mutations are a secondary event during the pathogenesis and progression of colorectal cancers. The expression and signaling activity differ among various *KRAS* mutants adding to the difficulty of developing drug regimens.

The identity of the tumor greatly impacts the response rate [29]. *RAS*-mutant pancreatic and colorectal cancers have a minimal response to inhibitors of the MAP kinase pathway. Similarly, clinical studies with sotorasib indicate that it is less effective in the treatment of *RAS*-mutant colorectal cancer than NSCLC. This suggests that the successful treatment of such colorectal cancers will require combination therapies to achieve a therapeutic response. As with many combination therapies, additive toxicities may prove problematic.

The intractability of *RAS*-driven tumors has led to the development of targeted covalent inhibitors (TCIs) of $KRAS^{G12C}$. Owing to toxicity and safety concerns, drugs that form irreversible covalent derivatives were disfavored as a drug class [93]. Aspirin, however, is a targeted covalent antagonist that has been in the therapeutic armamentarium since 1899. Roth et al. discovered that it exerts its therapeutic effect by acetylating serine 530 of COX1 (cyclooxygenase 1) [94,95]. Moreover, irreversible proton pump inhibitors such as omeprazole, esomeprazole, and lansoprazole that reduce stomach acid are effective, safe, and widely used in the treatment of dyspepsia, gastroesophageal reflux, and peptic ulcers [93]. That these three therapeutic agents are available to the public without a prescription indicates their measure of safety. These drugs react with an essential gastric proton pump (H^+/K^+ ATPase) cysteine to form an inactive disulfide adduct [96]. $KRAS^{G12C}$ is a natural target for a covalent inhibitor owing to the absence of an appropriate small-molecule binding pocket.

About 11.4% of all *RAS*-mutations (*KRAS, NRAS, HRAS*) are those of $KRAS^{G12C}$ [44]. In addition to the Michael acceptors such as acrylamide, warheads made of aziridines, activated acetylenes, epoxides, vinyl sulfones, and α-haloketones serve as irreversible inhibitors that react with cysteinyl residues [97,98]. In contrast, activated ketones, aldehydes, α-ketoheterocycles, α-ketoamides, α-cyanoacrylamide, cyanamide, carbonitriles, and boronic acid derivatives are warheads that function as reversible covalent protein-cysteine inhibitors. However, each of these agents along with sotorasib and adagrasib have the potential to target only about 10% of all *RAS* mutations ($KRAS^{G12C}$), leaving about 90% of mutations untargeted. This limitation calls for an expanded repertoire of warheads and drugs. Exon 2 mutations are the most common *KRAS* alteration and involve the conversion of glycine-12 to aspartate, valine, alanine, serine, arginine, or cysteine with mutation to aspartate, valine, and cysteine being the most common (Table 4). This calls for alternate strategies for blocking noncysteine mutations and such warheads have been developed. For example, *N*-methyl isoxazolium derivatives react with protein-aspartates, glutamates, and cysteine with aspartate being an important target in $KRAS^{G12D}$. Because this mutation makes up about one-third of *RAS* mutations, developing drugs that are directed against the G12D mutation is clinically important. Moreover, since the mutant aspartate is near the switch II pocket, it should be possible to design targeted covalent $KRAS^{G12D}$ inhibitors that are at least as effective in modifying the mutant protein as sotorasib.

Additional warheads have been designed that react with other amino acid residues found in proteins. For example, vinyl sulfones and vinyl sulfonamides form adducts with protein-lysines (and cysteines) while sulfonyl fluorides, sulfonimidoyl fluorides, and aryl fluorosulfates form adducts with protein-lysines (and tyrosines). Additionally, *N*-acyl-*N*-alkyl sulfonamides react with surface-exposed protein-lysines and 2-carbonylarylboronic acids are reversible inhibitors that attack protein-lysines. *RAS* mutations to lysine occur in NRAS and HRAS and represent potential targets of these chemical warheads. α-Cyanoacrylamide and α-cyanoenone warheads react reversibly with histidine (as found in the $KRAS^{Q61H}$ mutation). However, careful targeting will be required with these agents because they have the potential to react with many nonmutant target residues. Also in question is the possible existence of potential pockets in the region of mutations contiguous with the 13 and 61 positions of the RAS targets. See Ref. [98] for a comprehensive list and review of warhead classes, structures, and properties.

Targeted covalent inhibitors have arisen from the ranks of drugs to

be avoided to become an emerging paradigm. Much of this recent success can be attributed to the clinical efficacy of ibrutinib, a Bruton protein-tyrosine kinase (BTK) inhibitor that is used in the treatment of mantle cell lymphoma, chronic lymphocytic leukemia, Waldenstrom macroglobulinemia, and graph vs. host disease [99,100]. Moreover, the covalent inhibitor methodology has gained acceptance as a valuable component of the medicinal chemist's toolbox and is ready to make a substantial impact on the formulation of enzyme antagonists and receptor modulators [97] as demonstrated by the development and FDA-approval of sotorasib. The development of this first FDA-approved *RAS* mutant inhibitor represents a milestone in drug discovery. However, it is approved as a second-line treatment and it is not a panacea. There is a great need for the development of additional and more effective *RAS* mutant antagonists, perhaps as components of combination therapies.

Conflict of interest

The author is unaware of any affiliations, memberships, or financial holdings that might be perceived as affecting the objectivity of this review.

Acknowledgments

I thank Laura M. Roskoski for providing editorial and bibliographic assistance. I also acknowledge the assistance of Jasper Martinsek and Josie Rudnicki for their help in preparing the figures and W.S. Sheppard and Pasha Brezina for their help in structural analyses. The colored figures in this paper were evaluated to ensure that their perception was accurately conveyed to colorblind readers [101].

References

[1] A. Fernández-Medarde, J. De Las Rivas, E. Santos, 40 Years of RAS-a historic overview, Genes (2021) 681, https://doi.org/10.3390/genes12050681 (Basel).
[2] J.J. Harvey, An unidentified virus which causes the rapid production of tumours in mice, Nature 204 (1964) 1104–1105, https://doi.org/10.1038/2041104b0.
[3] W.H. Kirsten, L.A. Mayer, Malignant lymphomas of extrathymic origin induced in rats by murine erythroblastosis virus, J. Natl. Cancer Inst. 43 (1969) 735–746, https://doi.org/10.1093/jnci/39.2.311.
[4] M. Malumbres, M. Barbacid, RAS oncogenes: the first 30 years, Nat. Rev. Cancer 3 (2003) 459–465, https://doi.org/10.1038/nrc1097.
[5] E.H. Chang, M.A. Gonda, R.W. Ellis, E.M. Scolnick, D.R. Lowy, Human genome contains four genes homologous to transforming genes of Harvey and Kirsten murine sarcoma viruses, Proc. Natl. Acad. Sci. USA 79 (1982) 4848–4852, https://doi.org/10.1073/pnas.79.16.4848.
[6] G.M. Cooper, Cellular transforming genes, Science 217 (1982) 801–806, https://doi.org/10.1126/science.6285471.
[7] L.F. Parada, C.J. Tabin, C. Shih, R.A. Weinberg, Human EJ bladder carcinoma oncogene is homologue of Harvey sarcoma virus ras gene, Nature 297 (1982) 474–478, https://doi.org/10.1038/297474a0.
[8] E. Santos, S.R. Tronick, S.A. Aaronson, S. Pulciani, M. Barbacid, T24 human bladder carcinoma oncogene is an activated form of the normal human homologue of BALB- and Harvey-MSV transforming genes, Nature 298 (1982) 343–347, https://doi.org/10.1038/298343a0.
[9] E. Taparowsky, Y. Suard, O. Fasano, K. Shimizu, M. Goldfarb, M. Wigler, Activation of the T24 bladder carcinoma transforming gene is linked to a single amino acid change, Nature 300 (1982) 762–765, https://doi.org/10.1038/300762a0.
[10] C.J. Marshall, A. Hall, R.A. Weiss, A transforming gene present in human sarcoma cell lines, Nature 299 (1982) 171–173, https://doi.org/10.1038/299171a0.
[11] A. Hall, C.J. Marshall, N.K. Spurr, R.A. Weiss, Identification of transforming gene in two human sarcoma cell lines as a new member of the *ras* gene family located on chromosome 1, Nature 303 (1983) 396–400, https://doi.org/10.1038/303396a0.
[12] K. Shimizu, M. Goldfarb, M. Perucho, M. Wigler, Isolation and preliminary characterization of the transforming gene of a human neuroblastoma cell line, Proc. Natl. Acad. Sci. USA 80 (1983) 383–387, https://doi.org/10.1073/pnas.80.2.383.
[13] J.B. Gibbs, I.S. Sigal, M. Poe, E.M. Scolnick, Intrinsic GTPase activity distinguishes normal and oncogenic *ras* p21 molecules, Proc. Natl. Acad. Sci. USA 81 (1984) 5704–5708, https://doi.org/10.1073/pnas.81.18.5704.
[14] R. Roskoski Jr., RAF protein-serine/threonine kinases: structure and regulation, Biochem. Biophys. Res. Commun. 399 (2010) 313–317, https://doi.org/10.1016/j.bbrc.2010.07.092.
[15] R. Roskoski Jr., Targeting oncogenic Raf protein-serine/threonine kinases in human cancers, Pharmacol. Res. 135 (2018) 239–258, https://doi.org/10.1016/j.phrs.2018.08.013.
[16] R. Roskoski Jr., MEK1/2 dual-specificity protein kinases: structure and regulation, Biochem. Biophys. Res. Commun. 417 (2012) 5–10, https://doi.org/10.1016/j.bbrc.2011.11.145.
[17] R. Roskoski Jr., Allosteric MEK1/2 inhibitors including cobimetanib and trametinib in the treatment of cutaneous melanomas, Pharmacol. Res. 117 (2017) 20–31, https://doi.org/10.1016/j.phrs.2016.12.009.
[18] R. Roskoski Jr., ERK1/2 MAP kinases: structure, function, and regulation, Pharmacol. Res. 66 (2012) 105–143, https://doi.org/10.1016/j.phrs.2012.04.005.
[19] R. Roskoski Jr., Targeting ERK1/2 protein-serine/threonine kinases in human cancers, Pharmacol. Res. 142 (2019) 151–168, https://doi.org/10.1016/j.phrs.2019.01.039.
[20] L.M. Thorpe, H. Yuzugullu, J.J. Zhao, PI3K in cancer: divergent roles of isoforms, modes of activation and therapeutic targeting, Nat. Rev. Cancer 15 (2015) 7–24, https://doi.org/10.1038/nrc3860.
[21] F. Janku, T.A. Yap, F. Meric-Bernstam, Targeting the PI3K pathway in cancer: are we making headway? Nat. Rev. Clin. Oncol. 15 (2018) 273–291, https://doi.org/10.1038/nrclinonc.2018.28.
[22] M.N. Paddock, S.J. Field, L.C. Cantley, Treating cancer with phosphatidylinositol-3-kinase inhibitors: increasing efficacy and overcoming resistance, J. Lipid Res. 60 (2019) 747–752, https://doi.org/10.1194/jlr.S092130.
[23] G. Hoxhaj, B.D. Manning, The PI3K-AKT network at the interface of oncogenic signalling and cancer metabolism, Nat. Rev. Cancer 20 (2020) 74–88, https://doi.org/10.1038/s41568-019-0216-7.
[24] F. Sanchez-Vega, M. Mina, J. Armenia, W.K. Chatila, A. Luna, K.C. La, S. Dimitriadoy, D.L. Liu, H.S. Kantheti, S. Saghafinia, D. Chakravarty, F. Daian, Q. Gao, M.H. Bailey, W.W. Liang, S.M. Foltz, I. Shmulevich, L. Ding, Z. Heins, A. Ochoa, B. Gross, J. Gao, H. Zhang, R. Kundra, C. Kandoth, I. Bahceci, L. Dervishi, U. Dogrusoz, W. Zhou, H. Shen, P.W. Laird, G.P. Way, C.S. Greene, H. Liang, Y. Xiao, C. Wang, A. Iavarone, A.H. Berger, T.G. Bivona, A.J. Lazar, G. D. Hammer, T. Giordano, L.N. Kwong, G. McArthur, C. Huang, A.D. Tward, M. J. Frederick, F. McCormick, M. Meyerson, Cancer Genome Atlas Research Network, E.M. Van Allen, A.D. Cherniack, G. Ciriello, C. Sander, N. Schultz, Oncogenic signaling pathways in the cancer genome atlas, Cell 173 (2018) 321–337, https://doi.org/10.1016/j.cell.2018.03.035, e10.
[25] R. Roskoski Jr., Properties of FDA-approved small molecule phosphatidylinositol 3-kinase inhibitors prescribed for the treatment of malignancies, Pharmacol. Res. 168 (2021), 105579, https://doi.org/10.1016/j.phrs.2021.105579.
[26] F.C. Baltanás, N. Zarich, J.M. Rojas-Cabañeros, E. Santos, SOS GEFs in health and disease, Biochim. Biophys. Acta Rev. Cancer 1874 (2) (2020), 188445, https://doi.org/10.1016/j.bbcan.2020.188445.
[27] R. Roskoski Jr., The ErbB/HER family of protein-tyrosine kinases and cancer, Pharmacol. Res. 79 (2014) 34–74, https://doi.org/10.1016/j.phrs.2013.11.002.
[28] A.G. Stephen, D. Esposito, R.K. Bagni, F. McCormick, Dragging Ras back in the ring, Cancer Cell 25 (2014) 272–281, https://doi.org/10.1016/j.ccr.2014.02.017.
[29] D.K. Simanshu, D.V. Nissley, F. McCormick, RAS proteins and their regulators in human disease, Cell 170 (2017) 17–33, https://doi.org/10.1016/j.cell.2017.06.009.
[30] R.F. Dong, M.L. Zhu, M.M. Liu, Y.T. Xu, L.L. Yuan, J. Bian, Y.Z. Xia, L.Y. Kong, EGFR mutation mediates resistance to EGFR tyrosine kinase inhibitors in NSCLC: from molecular mechanisms to clinical research, Pharmacol. Res. 167 (2021), 105583, https://doi.org/10.1016/j.phrs.2021.105583.
[31] E.B. Ünal, F. Uhlitz, N. Blüthgen, A compendium of ERK targets, FEBS Lett. 591 (2017) 2607–2615, https://doi.org/10.1002/1873-3468.12740.
[32] T.F. Franke, D.R. Kaplan, L.C. Cantley, A. Toker, Direct regulation of the Akt proto-oncogene product by phosphatidylinositol-3,4-bisphosphate, Science 275 (1997) 665–668, https://doi.org/10.1126/science.275.5300.665.
[33] L. Braccini, E. Ciraolo, C.C. Campa, A. Perino, D.L. Longo, G. Tibolla, M. Pregnolato, Y. Cao, B. Tassone, F. Damilano, M. Laffargue, E. Calautti, M. Falasca, G.D. Norata, J.M. Backer, E. Hirsch, PI3K-C2γ is a Rab5 effector selectively controlling endosomal Akt2 activation downstream of insulin signalling, Nat. Commun. 6 (2015) 7400, https://doi.org/10.1038/ncomms8400.
[34] M. Whitman, C.P. Downes, M. Keeler, T. Keller, L. Cantley, Type I phosphatidylinositol kinase makes a novel inositol phospholipid, phosphatidylinositol-3-phosphate, Nature 332 (1988) 644–646, https://doi.org/10.1038/332644a0.
[35] A. Wallroth, V. Haucke, Phosphoinositide conversion in endocytosis and the endolysosomal system, J. Biol. Chem. 293 (2018) 1526–1535, https://doi.org/10.1074/jbc.R117.000629.
[36] A. Visentin, F. Frezzato, F. Severin, S. Imbergamo, S. Pravato, L. Romano Gargarella, S. Manni, S. Pizzo, E. Ruggieri, M. Facco, A.M. Brunati, G. Semenzato, F. Piazza, L. Trentin, Lights and shade of next-generation PI3K inhibitors in chronic lymphocytic leukemia, OncoTargets Ther. 13 (2020) 9679–9688, https://doi.org/10.2147/OTT.S268899, eCollection 2020.
[37] Z. Songyang, S.E. Shoelson, M. Chaudhuri, G. Gish, T. Pawson, W.G. Haser, F. King, T. Roberts, S. Ratnofsky, R.J. Lechleider, B.G. Neel, R.B. Birge, J. E. Fajardo, M.M. Chou, H. Hanafusa, B. Schaffhausen, L.C. Cantley, SH2 domains recognize specific phosphopeptide sequences, Cell 72 (1993) 767–778, https://doi.org/10.1016/0092-8674(93)90404-e.
[38] L.C. Cantley, Z. Songyang, Specificity in recognition of phosphopeptides by src-homology 2 domains, J. Cell Sci. Suppl. 18 (1994) 121–126, https://doi.org/10.1242/jcs.1994.supplement_18.18.

[39] M.D. Goncalves, B.D. Hopkins, L.C. Cantley, Phosphatidylinositol 3-kinase, growth disorders, and cancer, N. Engl. J. Med. 379 (2018) 2052–2062, https://doi.org/10.1056/NEJMra1704560.
[40] A. Hanlon, D.M. Brander, Managing toxicities of phosphatidylinositol-3-kinase (PI3K) inhibitors, Hematol. Am. Soc. Hematol. Educ. Program 2020 (2020) 346–356, https://doi.org/10.1182/hematology.2020000119.
[41] J.A. Engelman, Targeting PI3K signalling in cancer: opportunities, challenges and limitations, Nat. Rev. Cancer 9 (2009) 550–562, https://doi.org/10.1038/nrc2664.
[42] I.A. Prior, F.E. Hood, J.L. Hartley, The frequency of Ras mutations in cancer, Cancer Res. 80 (2020) 2969–2974, https://doi.org/10.1158/0008-5472.CAN-19-3682.
[43] K.Y. Seo, S.A. Jelinsky, E.L. Loechler, Factors that influence the mutagenic patterns of DNA adducts from chemical carcinogens, Mutat. Res. 463 (2000) 215–246, https://doi.org/10.1016/s1383-5742(00)00047-8.
[44] I. Khan, J.M. Rhett, J.P. O'Bryan, Therapeutic targeting of RAS: new hope for drugging the "undruggable", Biochim. Biophys. Acta Mol. Cell Res. 1867 (2020), 118570 https://doi.org/10.1016/j.bbamcr.2019.118570.
[45] R.L. Siegel, K.D. Miller, H.E. Fuchs, A. Jemal, Cancer statistics, 2021, CA Cancer J. Clin. 71 (2021) 7–33, https://doi.org/10.3322/caac.21654.
[46] C. Kandoth, M.D. McLellan, F. Vandin, K. Ye, B. Niu, C. Lu, M. Xie, Q. Zhang, J. F. McMichael, M.A. Wyczalkowski, M.D.M. Leiserson, C.A. Miller, J.S. Welch, M. J. Walter, M.C. Wendl, T.J. Ley, R.K. Wilson, B.J. Raphael, L. Ding, Mutational landscape and significance across 12 major cancer types, Nature 502 (2013) 333–339, https://doi.org/10.1038/nature12634.
[47] Y. Zhang, P. Kwok-Shing Ng, M. Kucherlapati, F. Chen, Y. Liu, Y.H. Tsang, G. de Velasco, K.J. Jeong, R. Akbani, A. Hadjipanayis, A. Pantazi, C.A. Bristow, E. Lee, H.S. Mahadeshwar, J. Tang, J. Zhang, L. Yang, S. Seth, S. Lee, X. Ren, X. Song, H. Sun, J. Seidman, L.J. Luquette, R. Xi, L. Chin, A. Protopopov, T.F. Westbrook, C.S. Shelley, T.K. Choueiri, M. Ittmann, C. Van Waes, J.N. Weinstein, H. Liang, E. P. Henske, A.K. Godwin, P.J. Park, R. Kucherlapati, K.L. Scott, G.B. Mills, D. J. Kwiatkowski, C.J. Creighton, A pan-cancer proteogenomic atlas of PI3K/AKT/mTOR pathway alterations, Cancer Cell 31 (2017) 820–832, https://doi.org/10.1016/j.ccell.2017.04.013, e3.
[48] R. Roskoski Jr., ErbB/HER protein-tyrosine kinases: structure and small molecule inhibitors, Pharmacol. Res. 87 (2014) 42–59, https://doi.org/10.1016/j.phrs.2014.06.001.
[49] R. Roskoski Jr., Small molecule inhibitors targeting the EGFR/ErbB family of protein-tyrosine kinases in human cancers, Pharmacol. Res. 139 (2019) 395–411, https://doi.org/10.1016/j.phrs.2018.11.014.
[50] R. Roskoski Jr., Properties of FDA-approved small molecule protein kinase inhibitors, Pharmacol. Res. 144 (2019) 19–50, https://doi.org/10.1016/j.phrs.2019.03.006.
[51] T. Pantsar, The current understanding of KRAS protein structure and dynamics, Comput. Struct. Biotechnol. J. 18 (2019) 189–198, https://doi.org/10.1016/j.csbj.2019.12.004, eCollection 2020.
[52] M.V. Milburn, L. Tong, A.M. deVos, A. Brünger, Z. Yamaizumi, S. Nishimura, S. H. Kim, Molecular switch for signal transduction: structural differences between active and inactive forms of protooncogenic ras proteins, Science 247 (1990) 939–945, https://doi.org/10.1126/science.2406906.
[53] D. Rabara, T.H. Tran, S. Dharmaiah, R.M. Stephens, F. McCormick, D. K. Simanshu, M. Holderfield, KRAS G13D sensitivity to neurofibromin-mediated GTP hydrolysis, Proc. Natl. Acad. Sci. USA 116 (2019) 22122–22131, https://doi.org/10.1073/pnas.1908353116.
[54] K. Scheffzek, G. Shivalingaiah, Ras-specific GTPase-activating proteins-structures, mechanisms, and interactions, Cold Spring Harb. Perspect. Med. 9 (2019), a031500, https://doi.org/10.1101/cshperspect.a031500.
[55] J.M. Ostrem, U. Peters, M.L. Sos, J.A. Wells, K.M. Shokat, K-Ras(G12C) inhibitors allosterically control GTP affinity and effector interactions, Nature 503 (7477) (2013 28) 548–551, https://doi.org/10.1038/nature12796.
[56] B.A. Lanman, J.R. Allen, J.G. Allen, A.K. Amegadzie, K.S. Ashton, S.K. Booker, J. J. Chen, N. Chen, M.J. Frohn, G. Goodman, D.J. Kopecky, L. Liu, P. Lopez, J. D. Low, V. Ma, A.E. Minatti, T.T. Nguyen, N. Nishimura, A.J. Pickrell, A.B. Reed, Y. Shin, A.C. Siegmund, N.A. Tamayo, C.M. Tegley, M.C. Walton, H.L. Wang, R. P. Wurz, M. Xue, K.C. Yang, P. Achanta, M.D. Bartberger, J. Canon, L.S. Hollis, J. D. McCarter, C. Mohr, K. Rex, A.Y. Saiki, T. San Miguel, L.P. Volak, K.H. Wang, D. A. Whittington, S.G. Zech, J.R. Lipford, V.J. Cee, Discovery of a covalent inhibitor of KRAS G12C (AMG 510) for the treatment of solid tumors, J. Med. Chem. 63 (2020) 52–65, https://doi.org/10.1021/acs.jmedchem.9b01180.
[57] C.A. Lipinski, F. Lombardo, B.W. Dominy, P.J. Feeney, Experimental and computational approaches to estimate solubility and permeability in drug discovery and development settings, Adv. Drug Deliv. Rev. 46 (2001) 3–26, https://doi.org/10.1016/s0169-409x(00)00129-0.
[58] D.S. Hong, M.G. Fakih, J.H. Strickler, J. Desai, G.A. Durm, G.I. Shapiro, G. S. Falchook, T.J. Price, A. Sacher, C.S. Denlinger, Y.J. Bang, G.K. Dy, J.C. Krauss, Y. Kuboki, J.C. Kuo, A.L. Coveler, K. Park, T.W. Kim, F. Barlesi, P.N. Munster, S. S. Ramalingam, T.F. Burns, F. Meric-Bernstam, H. Henary, J. Ngang, G. Ngarmchamnanrith, J. Kim, B.E. Houk, J. Canon, J.R. Lipford, G. Friberg, P. Lito, R. Govindan, B.T. Li, KRAS G12C inhibition with sotorasib in advanced solid tumors, N. Engl. J. Med. 383 (2020) 1207–1217, https://doi.org/10.1056/NEJMoa1917239.
[59] F. Skoulidis, B.T. Li, G.K. Dy, T.J. Price, G.S. Falchook, J. Wolf, A. Italiano, M. Schuler, H. Borghaei, F. Barlesi, T. Kato, A. Curioni-Fontecedro, A. Sacher, A. Spira, S.S. Ramalingam, T. Takahashi, B. Besse, A. Anderson, A. Ang, Q. Tran, O. Mather, H. Henary, G. Ngarmchamnanrith, G. Friberg, V. Velcheti, R. Govindan, Sotorasib for lung cancers with KRAS p.G12C mutation, N. Engl. J. Med. 384 (2021) 2371–2381, https://doi.org/10.1056/NEJMoa2103695.
[60] A. Indini, E. Rijavec, M. Ghidini, A. Cortellini, F. Grossi, Targeting KRAS in solid tumors: current challenges and future opportunities of novel KRAS inhibitors, Pharmaceutics 13 (2021) 653, https://doi.org/10.3390/pharmaceutics13050653.
[61] J.B. Fell, J.P. Fischer, B.R. Baer, J.F. Blake, K. Bouhana, D.M. Briere, K.D. Brown, L.E. Burgess, A.C. Burns, M.R. Burkard, H. Chiang, M.J. Chicarelli, A.W. Cook, J. J. Gaudino, J. Hallin, L. Hanson, D.P. Hartley, E.J. Hicken, G.P. Hingorani, R. J. Hinklin, M.J. Mejia, P. Olson, J.N. Otten, S.P. Rhodes, M.E. Rodriguez, P. Savechenkov, D.J. Smith, N. Sudhakar, F.X. Sullivan, T.P. Tang, G.P. Vigers, L. Wollenberg, J.G. Christensen, M.A. Marx, Identification of the clinical development candidate MRTX849, a covalent KRAS^{G12C} inhibitor for the treatment of cancer, J. Med. Chem. 63 (2020) 6679–6693, https://doi.org/10.1021/acs.jmedchem.9b02052.
[62] M.M. Awad, S. Liu, I.I. Rybkin, K.C. Arbour, J. Dilly, V.W. Zhu, M.L. Johnson, R. S. Heist, T. Patil, G.J. Riely, J.O. Jacobson, X. Yang, N.S. Persky, D.E. Root, K. E. Lowder, H. Feng, S.S. Zhang, K.M. Haigis, Y.P. Hung, L.M. Sholl, B.M. Wolpin, J. Wiese, J. Christiansen, J. Lee, A.B. Schrock, L.P. Lim, K. Garg, M. Li, L. D. Engstrom, L. Waters, J.D. Lawson, P. Olson, P. Lito, S.I. Ou, J.G. Christensen, P. A. Jänne, A.J. Aguirre, Acquired resistance to KRAS^{G12C} inhibition in cancer, N. Engl. J. Med. 384 (2021) 2382–2393, https://doi.org/10.1056/NEJMoa2105281.
[63] R. Roskoski Jr., Properties of FDA-approved small molecule protein kinase inhibitors: a 2020 update, Pharmacol. Res. 152 (2020), 104609, https://doi.org/10.1016/j.phrs.2019.104609.
[64] A.R. Moore, S.C. Rosenberg, F. McCormick, S. Malek, RAS-targeted therapies: is the undruggable drugged? Nat. Rev. Drug Discov. 19 (2020) 533–552, https://doi.org/10.1038/s41573-020-0068-6.
[65] R. Roskoski Jr., Protein prenylation: a pivotal posttranslational process, Biochem. Biophys. Res. Commun. 303 (2003) 1–7, https://doi.org/10.1016/s0006-291x(03)00323-1.
[66] N. Berndt, A.D. Hamilton, S.M. Sebti, Targeting protein prenylation for cancer therapy, Nat. Rev. Cancer 11 (2011) 775–791, https://doi.org/10.1038/nrc3151.
[67] R. Roskoski Jr., P. Ritchie, Role of the carboxyterminal residue in peptide binding to protein farnesyltransferase and protein geranylgeranyltransferase, Arch. Biochem. Biophys. 356 (1998) 167–176, https://doi.org/10.1006/abbi.1998.0768.
[68] T.B. Karasic, E.G. Chiorean, S.M. Sebti, P.J. O'Dwyer, A phase I study of GGTI-2418 (geranylgeranyl transferase I inhibitor) in patients with advanced solid tumors, Target Oncol. 14 (2019) 613–618, https://doi.org/10.1007/s11523-019-00661-5.
[69] R. Roskoski Jr., A historical overview of protein kinases and their targeted small molecule inhibitors, Pharmacol. Res. 100 (2015) 1–23, https://doi.org/10.1016/j.phrs.2015.07.010.
[70] R. Roskoski Jr., Properties of FDA-approved small molecule protein kinase inhibitors: a 2021 update, Pharmacol. Res. 165 (2021), 105463, https://doi.org/10.1016/j.phrs.2021.105463.
[71] R. Roskoski Jr., The role of small molecule kit protein-tyrosine kinase inhibitors in the treatment of neoplastic disorders, Pharmacol. Res. 133 (2018) 35–52, https://doi.org/10.1016/j.phrs.2018.04.020.
[72] A. Adenis, T. Mazard, J. Fraisse, P. Chalbos, B. Pastor, L. Evesque, F. Ghiringhelli, C. Mollevi, S. Delaine, M. Ychou, FOLFIRINOX-R study design: a phase I/II trial of FOLFIRINOX plus regorafenib as first line therapy in patients with unresectable RAS-mutated metastatic colorectal cancer, BMC Cancer 21 (2021) 564, https://doi.org/10.1186/s12885-021-08312-7.
[73] D. Uprety, A.A. Adjei, KRAS: from undruggable to a druggable cancer target, Cancer Treat. Rev. 89 (2020), 102070, https://doi.org/10.1016/j.ctrv.2020.102070.
[74] I. Yen, F. Shanahan, M. Merchant, C. Orr, T. Hunsaker, M. Durk, H. La, X. Zhang, S.E. Martin, E. Lin, J. Chan, Y. Yu, D. Amin, R.M. Neve, A. Gustafson, A. Venkatanarayan, S.A. Foster, J. Rudolph, C. Klijn, S. Malek, Pharmacological induction of RAS-GTP confers RAF inhibitor sensitivity in KRAS mutant tumors, Cancer Cell 34 (2018) 611–625, https://doi.org/10.1016/j.ccell.2018.09.002, e7.
[75] M. Xie, X. Xu, Y. Fan, KRAS-mutant non-small cell lung cancer: an emerging promisingly treatable subgroup, Front. Oncol. 11 (2021), 672612, https://doi.org/10.3389/fonc.2021.672612 eCollection 2021.
[76] R. Roskoski Jr., A. Sadeghi-Nejad, Role of RET protein-tyrosine kinase inhibitors in the treatment RET-driven thyroid and lung cancers, Pharmacol. Res. 128 (2018) 1–17, https://doi.org/10.1016/j.phrs.2017.12.021.
[77] R. Roskoski Jr., The role of small molecule platelet-derived growth factor receptor (PDGFR) inhibitors in the treatment of neoplastic disorders, Pharmacol. Res. 129 (2018) 65–83, https://doi.org/10.1016/j.phrs.2018.01.021.
[78] V. Papadimitrakopoulou, J.J. Lee, I.I. Wistuba, A.S. Tsao, F.V. Fossella, N. Kalhor, S. Gupta, L.A. Byers, J.G. Izzo, S.N. Gettinger, S.B. Goldberg, X. Tang, V.A. Miller, F. Skoulidis, D.L. Gibbons, L. Shen, C. Wei, L. Diao, S.A. Peng, J. Wang, A.L. Tam, K.R. Coombes, J.S. Koo, D.J. Mauro, E.H. Rubin, J.V. Heymach, W.K. Hong, R. S. Herbst, The BATTLE-2 study: a biomarker-integrated targeted therapy study in previously treated patients with advanced non-small-cell lung cancer, J. Clin. Oncol. 34 (2016) 3638–3647, https://doi.org/10.1200/JCO.2015.66.0084.
[79] J. Desai, H. Gan, C. Barrow, M. Jameson, V. Atkinson, A. Haydon, M. Millward, S. Begbie, M. Brown, B. Markman, W. Patterson, A. Hill, L. Horvath, A. Nagrial, G. Richardson, C. Jackson, M. Friedlander, P. Parente, B. Tran, L. Wang, Y. Chen, Z. Tang, W. Huang, J. Wu, D. Zeng, L. Luo, B. Solomon, Phase I, open-label, dose-escalation/dose-expansion study of lifirafenib (BGB-283), an RAF family kinase

inhibitor, in patients with solid tumors, J. Clin. Oncol. 38 (2020) 2140–2150, https://doi.org/10.1200/JCO.19.02654.
[80] R. Roskoski Jr., Hydrophobic and polar interactions of FDA-approved small molecule protein kinase inhibitors with their target enzymes, Pharmacol. Res. 169 (2021), 105660, https://doi.org/10.1016/j.phrs.2021.105660.
[81] P.A. Jänne, M.M. van den Heuvel, F. Barlesi, M. Cobo, J. Mazieres, L. Crinò, S. Orlov, F. Blackhall, J. Wolf, P. Garrido, A. Poltoratskiy, G. Mariani, D. Ghiorghiu, E. Kilgour, P. Smith, A. Kohlmann, D.J. Carlile, D. Lawrence, K. Bowen, J. Vansteenkiste, Selumetinib plus docetaxel compared with docetaxel alone and progression-free survival in patients with *KRAS*-mutant advanced non-small cell lung cancer: the SELECT-1 randomized clinical trial, JAMA 317 (2017) 1844–1853, https://doi.org/10.1001/jama.2017.3438.
[82] G.R. Blumenschein Jr., E.F. Smit, D. Planchard, D.W. Kim, J. Cadranel, T. De Pas, F. Dunphy, K. Udud, M.J. Ahn, N.H. Hanna, J.H. Kim, J. Mazieres, S.W. Kim, P. Baas, E. Rappold, S. Redhu, A. Puski, F.S. Wu, P.A. Jänne, A randomized phase II study of the MEK1/MEK2 inhibitor trametinib (GSK1120212) compared with docetaxel in *KRAS*-mutant advanced non-small-cell lung cancer (NSCLC), Ann. Oncol. 26 (2015) 894–901, https://doi.org/10.1093/annonc/mdv072.
[83] E. Martinelli, F. Morgillo, T. Troiani, F. Ciardiello, Cancer resistance to therapies against the EGFR-RAS-RAF pathway: the role of MEK, Cancer Treat. Rev. 53 (2017) 61–69, https://doi.org/10.1016/j.ctrv.2016.12.001.
[84] H.Y. Lim, J. Heo, H.J. Choi, C.Y. Lin, J.H. Yoon, C. Hsu, K.M. Rau, R.T. Poon, W. Yeo, J.W. Park, M.H. Tay, W.S. Hsieh, C. Kappeler, P. Rajagopalan, H. Krissel, M. Jeffers, C.J. Yen, W.Y. Tak, A phase II study of the efficacy and safety of the combination therapy of the MEK inhibitor refametinib (BAY 86-9766) plus sorafenib for Asian patients with unresectable hepatocellular carcinoma, Clin. Cancer Res. 20 (2014) 5976–5985, https://doi.org/10.1158/1078-0432.CCR-13-3445.
[85] M. Martinez-Garcia, U. Banerji, J. Albanell, R. Bahleda, S. Dolly, F. Kraeber-Bodéré, F. Rojo, E. Routier, E. Guarin, Z.X. Xu, R. Rueger, J.J. Tessier, E. Shochat, S. Blotner, V.M. Naegelen, J.C. Soria, First-in-human, phase I dose-escalation study of the safety, pharmacokinetics, and pharmacodynamics of RO5126766, a first-in-class dual MEK/RAF inhibitor in patients with solid tumors, Clin. Cancer Res. 18 (2012) 4806–4819, https://doi.org/10.1158/1078-0432.CCR-12-0742.
[86] C. Guo, M. Chénard-Poirier, D. Roda, M. de Miguel, S.J. Harris, I.M. Candilejo, P. Sriskandarajah, W. Xu, M. Scaranti, A. Constantinidou, J. King, M. Parmar, A. J. Turner, S. Carreira, R. Riisnaes, L. Finneran, E. Hall, Y. Ishikawa, K. Nakai, N. Tunariu, B. Basu, M. Kaiser, J.S. Lopez, A. Minchom, J.S. de Bono, U. Banerji, Intermittent schedules of the oral RAF-MEK inhibitor CH5126766/VS-6766 in patients with *RAS/RAF*-mutant solid tumours and multiple myeloma: a single-centre, open-label, phase 1 dose-escalation and basket dose-expansion study, Lancet Oncol. 21 (2020) 1478–1488, https://doi.org/10.1016/S1470-2045(20)30464-2.
[87] K. Chen, Y. Zhang, L. Qian, P. Wang, Emerging strategies to target RAS signaling in human cancer therapy, J. Hematol. Oncol. 14 (1) (2021) 116, https://doi.org/10.1186/s13045-021-01127-w.
[88] R.J. Sullivan, J.R. Infante, F. Janku, D.J.L. Wong, J.A. Sosman, V. Keedy, M. R. Patel, G.I. Shapiro, J.W. Mier, A.W. Tolcher, A. Wang-Gillam, M. Sznol, K. Flaherty, E. Buchbinder, R.D. Carvajal, A.M. Varghese, M.E. Lacouture, A. Ribas, S.P. Patel, G.A. DeCrescenzo, C.M. Emery, A.L. Groover, S. Saha, M. Varterasian, D.J. Welsch, D.M. Hyman, B.T. Li, First-in-class ERK1/2 inhibitor ulixertinib (BVD-523) in patients with MAPK mutant advanced solid tumors: results of a phase I dose-escalation and expansion study, Cancer Discov. 8 (2018) 184–195, https://doi.org/10.1158/2159-8290.CD-17-1119.
[89] A. Bardia, M. Gounder, J. Rodon, F. Janku, M.P. Lolkema, J.J. Stephenson, P. L. Bedard, M. Schuler, C. Sessa, P. LoRusso, M. Thomas, H. Maacke, H. Evans, Y. Sun, D.S.W. Tan, Phase Ib study of combination therapy with MEK inhibitor binimetinib and phosphatidylinositol 3-kinase inhibitor buparlisib in patients with advanced solid tumors with RAS/RAF alterations, Oncologist 25 (2020) e160–e169, https://doi.org/10.1634/theoncologist.2019-0297.
[90] J.R. Brahmer, S.S. Tykodi, L.Q. Chow, W.J. Hwu, S.L. Topalian, P. Hwu, C. G. Drake, L.H. Camacho, J. Kauh, K. Odunsi, H.C. Pitot, O. Hamid, S. Bhatia, R. Martins, K. Eaton, S. Chen, T.M. Salay, S. Alaparthy, J.F. Grosso, A.J. Korman, S.M. Parker, S. Agrawal, S.M. Goldberg, D.M. Pardoll, A. Gupta, J.M. Wigginton, Safety and activity of anti-PD-L1 antibody in patients with advanced cancer, N. Engl. J. Med. 366 (2012) 2455–2465, https://doi.org/10.1056/NEJMoa1200694.
[91] R. Cristescu, R. Mogg, M. Ayers, A. Albright, E. Murphy, J. Yearley, X. Sher, X. Q. Liu, H. Lu, M. Nebozhyn, C. Zhang, J.K. Lunceford, A. Joe, J. Cheng, A. L. Webber, N. Ibrahim, E.R. Plimack, P.A. Ott, T.Y. Seiwert, A. Ribas, T. K. McClanahan, J.E. Tomassini, A. Loboda, D. Kaufman, Pan-tumor genomic biomarkers for PD-1 checkpoint blockade-based immunotherapy, Science 362 (2018), eaar3593, https://doi.org/10.1126/science.aar3593.
[92] S.A. Kerk, T. Papagiannakopoulos, Y.M. Shah, C.A. Lyssiotis, Metabolic networks in mutant KRAS-driven tumours: tissue specificities and the microenvironment, Nat. Rev. Cancer 21 (2021) 510–525, https://doi.org/10.1038/s41568-021-00375-9.
[93] J. Singh, R.C. Petter, T.A. Baillie, A. Whitty, The resurgence of covalent drugs, Nat. Rev. Drug Discov. 10 (2011) 307–317, https://doi.org/10.1038/nrd3410.
[94] G.J. Roth, N. Stanford, P.W. Majerus, Acetylation of prostaglandin synthase by aspirin, Proc. Natl. Acad. Sci. USA 72 (1975) 3073–3076, https://doi.org/10.1073/pnas.72.8.3073.
[95] R.M. Botting, Vane's discovery of the mechanism of action of aspirin changed our understanding of its clinical pharmacology, Pharmacol. Rep. 62 (2010) 518–525, https://doi.org/10.1016/s1734-1140(10)70308-x.
[96] R.M. Ward, G.L. Kearns, Proton pump inhibitors in pediatrics: mechanism of action, pharmacokinetics, pharmacogenetics, and pharmacodynamics, Paediatr. Drugs 15 (2013) 119–131, https://doi.org/10.1007/s40272-013-0012-x.
[97] T.A. Baillie, Targeted covalent inhibitors for drug design, Angew. Chem. Int. Ed. 55 (2016) 13408–13421, https://doi.org/10.1002/anie.201601091.
[98] M. Gehringer, S.A. Laufer, Emerging and re-emerging warheads for targeted covalent inhibitors: applications in medicinal chemistry and chemical biology, J. Med. Chem. 62 (2019) 5673–5724, https://doi.org/10.1021/acs.jmedchem.8b01153.
[99] R. Roskoski Jr., Orally effective FDA-approved protein kinase targeted covalent inhibitors (TCIs), Pharmacol. Res. 165 (2021), 105422, https://doi.org/10.1016/j.phrs.2021.105422.
[100] R. Roskoski Jr., Ibrutinib inhibition of bruton protein-tyrosine kinase (BTK) in the treatment of B cell neoplasms, Pharmacol. Res. 113 (Pt. A) (2016) 395–408, https://doi.org/10.1016/j.phrs.2016.09.011.
[101] R. Roskoski Jr., Guidelines for preparing color figures for everyone including the colorblind, Pharmacol. Res. 119 (2017) 240–241, https://doi.org/10.1016/j.phrs.2017.02.005. Corrigendum: doi: 10.1016/j.phrs.2018.09.019.